HHS Public Access

Author manuscript

Nat Rev Bioeng. Author manuscript; available in PMC 2024 August 30.

Published in final edited form as:

Nat Rev Bioeng. 2023 March ; 1(3): 193–207. doi:10.1038/s44222-023-00022-y.

Neural modulation with photothermally active nanomaterials

Yingqiao Wang[1,4], **Raghav Garg**[1,4], **Devora Cohen-Karni**[2], **Tzahi Cohen-Karni**[1,3]

[1]Department of Materials Science and Engineering, Carnegie Mellon University, Pittsburgh, PA, USA.

[2]Preclinical education biochemistry, Lake Erie College of Osteopathic Medicine at Seton Hill, Greensburg, PA, USA.

[3]Department of Biomedical Engineering, Carnegie Mellon University, Pittsburgh, PA, USA.

[4]These authors contributed equally: Yingqiao Wang, Raghav Garg.

Abstract

Modulating neural electrophysiology with high precision is essential for understanding neural communication and for the diagnosis and treatment of neural disorders. Photothermal modulation offers a remote and non-genetic method for neural modulation with high spatiotemporal resolution and specificity. This technique induces highly localized and transient temperature changes at the cell membrane interfaced with photothermally active nanomaterials. This rapid temperature change affects the electrical properties of the cell membrane or temperature-sensitive ion channels. In this Review, we discuss the fundamental material properties and illumination conditions that are necessary for nanomaterial-assisted photothermal neural excitation and inhibition. We examine how this versatile technique allows direct investigation of neural electrophysiology and signalling pathways in two-dimensional and three-dimensional cell cultures and tissues, and highlight the scientific and technological challenges in terms of cellular specificity, light delivery and biointerface stability on the road to clinical translation.

Introduction

Understanding the complex electrophysiology of interconnected biological neural circuits for the treatment of neurological diseases requires neural electrophysiology modulation techniques with subcellular resolution[1,2]. Nanomaterials and microfabrication techniques

Correspondence should be addressed to Tzahi Cohen-Karni. tzahi@andrew.cmu.edu.

Author contributions

Y.W. and R.G. contributed equally to this work.

Competing interests

The authors declare that they have no known competing financial interests or personal relationships that could have appeared to influence the work reported in this paper.

Additional information

Supplementary information The online version contains supplementary material available at https://doi.org/10.1038/s44222-023-00022-y.

Peer review information *Nature Reviews Bioengineering* thanks Guosong Hong, Diego Ghezzi, and the other, anonymous, reviewer for their contribution to the peer review of this work.

have enabled the development of implantable bioelectronics with stable biointerfaces and high spatiotemporal resolution to record and modulate electrophysiological activities[3–9]. Such bioelectronics allowed the establishment of correlations between electrophysiology and higher-order functions in healthy and diseased states, for example, identifying the role of the subthalamic nucleus in motor control and Parkinson disease[10], and the development of therapeutics to restore lost sensing functionalities[2,11,12]. However, bioelectronics lack cell type specificity and require invasive implantation, resulting in acute and chronic side effects on the interfaced cells and tissues[13–17].

Optogenetics can facilitate optical control of cellular activity by genetically introducing light-sensitive proteins in target cells and tissues[18]; for example, optogenetic therapy has been applied for the partial recovery of visual function in a blind patient with retinitis pigmentosa (NCT03326336)[19]. However, the clinical translation of optogenetics has been restricted owing to ethical and safety considerations of the genetic modification[18,20,21]. Alternatively, direct illumination of the cell membrane with infrared-light pulses can induce cell membrane depolarization without the need for genetic transfection[22–24]. However, this technique lacks cellular specificity, has low spatial resolution (especially at subcellular dimensions), and requires high incident energy that may damage the target cells and tissues[25–27].

Nanomaterials that can efficiently convert external stimuli, such as incident magnetic and electromagnetic signals, into localized thermal and electrical changes can reduce the required incident energy and facilitate targeted neural modulation[14,28–31]; for example, magnetogenetics allows the targeted excitation of cells interfaced with superparamagnetic nanoparticles such as iron oxide nanoparticles[30]. Under alternating magnetic fields, superparamagnetic nanoparticles dissipate thermal energy owing to hysteresis[30,32]. Localizing temperature increase to the membrane of cells expressing temperature-activated transient receptor potential (TRP) ion channels leads to TRP activation and subsequent cellular depolarization[30,33]. By targeting the TRP ankyrin 1 (TRPA1) somatosensory ion channel, sub-second magnetothermal neuromodulation in *Drosophila melanogaster* has been achieved[32]. However, magnetogenetics requires genetic modifications of target cells and tissues to achieve TRP overexpression, which limits its clinical translation. Alternatively, optoelectronic nanomaterials, such as heterojunction semiconducting Si nanowires (SiNWs) and polymers, convert incident photons into electrons (or holes) for photoelectric and photoelectrochemical neuromodulation[14,34–36]. Incident electromagnetic radiation induces charge separation in these nanomaterials, leading to localized electric currents that depolarize the interfaced cell membrane[37]. However, despite their long-term stability, the potential toxic byproducts of photocatalytic reactions may hinder clinical translation.

Photothermally active materials rapidly convert incident electromagnetic radiation into localized thermal energy[38]; for example, plasmonic nanoparticles[39], multidimensional nanocarbons[29], inorganic Si-based nanostructures[31,37], two-dimensional (2D) nanosheets and polymer-based nanomaterials[40,41]. The rapid local temperature increase in the proximity of cells affects the properties of the cell membrane, leading to photothermal modulation of cellular processes, including electrophysiology (excitation and inhibition) and signalling

pathways[42,43], and allowing remote, non-genetic and non-catalytic control over neural activity.

In this Review, we discuss the mechanisms and material properties (optical absorption, photothermal energy conversion and biocompatibility) necessary for efficient photothermal modulation. We discuss biointerfaces across multiple dimensions, from single cells to tissues and animal models, and consider the specific structural, chemical and compositional alterations for safe and high-efficiency neuromodulation. We present applications of photothermal modulation, including direct control of neural excitation and inhibition, and discuss synergetic multidisciplinary approaches and clinical translation of neural regeneration[9,14,19,44–46] as well as new photothermal therapeutics for neural disorders such as Parkinson disease[47] and epilepsy[48].

Mechanisms of photothermal modulation

The cell membrane plays an important role in regulating cellular activity and communication[49]. To achieve photothermal modulation of a neuron, nanomaterials must be closely interfaced with the cell membrane (Fig. 1a). Illuminating the biointerface between nanomaterials and neurons leads to a local release of thermal energy that directly affects neuron membrane functionality[42,43,50–52]. Two mechanisms have been proposed for photothermal modulation: change in neuron membrane capacitance and resistance, and activation of membrane temperature-sensitive ion channels[42,43,50–53]. The relative contribution of each mechanism depends on the cell type, physical properties of the biointerface (for example, specific or non-specific binding of the nanomaterial to the cell membrane) and illumination conditions (for example, light pulse duration and power).

The cell membrane can be modelled as a combination of electrical circuit elements, that are, resistive element ($R_m(T)$), capacitive element ($C_m(T)$) and batteries (net surface potential V_s and resting potential V_r)[49] (Box 1 and Fig. 1a). This model can explain the generation of action potential during neural activation as a result of transmembrane current[49]. Building on this model, an optocapacitive mechanism was proposed to explain the photothermal modulation of neurons[42,43,51]. Here, a rapid increase in local temperature induces a change in cell membrane capacitance leading to membrane depolarization[42,43] (Fig. 1a), where the membrane capacitance is a linear function of the induced temperature change as described by:

$$C_m(T) = C_0 + \alpha(T - T_0) \quad (1)$$

where C_0, α and T_0 are cell membrane capacitance at resting potential, capacitance change per unit change in temperature and ambient temperature, respectively[42,43,51]. A change in the local temperature directly changes the membrane capacitance irrespective of temperature-sensitive ion channels[42,43]. This induces a capacitive current (i_c) across the cell membrane as described by:

$$i_c = C_m(T)\frac{dV}{dt} + (V - V_s)\frac{dC_m(T)}{dt} \quad (2)$$

where V and V_s are the membrane potential and the net surface potential of the membrane, respectively[42,43]. From equations (1) and (2), it can be determined that the capacitive current through the cell membrane is a function of the temperature gradient dT/dt. To induce an action potential, the magnitude of dT/dt should be large enough such that the generated capacitive current is greater than the excitation threshold[42,43]. Mechanoelectrical thermal activation can be an alternative mechanism for photothermal excitation[22], and suggests that localized temperature transients cause physical expansion of the plasma membrane, which in turn generate the depolarizing current[22].

Inhibition of neural activity can also be achieved through photothermal techniques[50,52,54]. Here, the localized temperature transients are leveraged to affect cell membrane resistance[50,52]. The temperature dependence of the resistive element of the cell membrane can be described by:

$$R_m(T) = R_0 Q_{10}^{-\frac{(T - T_0)}{10}} \quad (3)$$

where R_0, T_0 and Q_{10} are the cell membrane resistance at resting potential, the ambient temperature and the change in the rate of activity resulting from an increase in temperature of 10 °C, respectively[50]. A substantial temperature increase therefore induces a change in membrane resistance, generating a transmembrane current from the outside to the inside of the neuron and resulting in membrane hyperpolarization[50].

Alternatively, control of neural activity can be achieved through control of ion channel response. Temperature-sensitive channels, such as TRP ion channels, can be activated at elevated temperatures[55]. When the external temperature is greater than the threshold of a temperature-sensitive ion channel (~42 °C for TRP vanilloid 1 (TRPV1)), the channel actively opens, leading to an ionic flux through the membrane (for example, Ca^{2+} influx for TRPV1). Conjugating photothermal agents in proximity to such ion channels localizes the temperature increase and leads to the induction of a transmembrane current through the channel[51,53] (Fig. 1a).

These mechanisms illustrate multiple pathways for neural excitation and inhibition (Fig. 1b). Beyond the modulation of electrophysiology activities, endocytosis of the nanomaterials can further alter gene expression and signalling pathways inside interfaced neurons (Fig. 1b).

Photothermally active nanomaterials

Multidimensionality—Nanomaterials have numerous properties advantageous for photothermal modulation, including a high surface area to volume ratio, enhanced optical absorption and energy conversion, and ease of functionalization[56,57]. The structure and

dimensionality of nanomaterials directly affect their properties and can be tailored to specific biomedical applications such as chemical sensing, drug delivery, bioelectronics and photothermal therapy[7,56–58]. In particular, their nanoscale dimension enables biointerfaces with high spatial resolution[59], and their multidimensionality allows the design of biointerfaces at different scales — from the subcellular scale to in vivo animal models[56,57] (Fig. 1c).

Au nanoparticles (AuNPs) have been widely studied for biomedical applications such as drug delivery, immunohistochemistry, cancer therapy andphotothermalmodulation[60,61]. AuNPs have well-established synthesis protocols and tunable optical and photothermal energy conversion properties[39,62]. In addition to AuNPs, other photothermally active zero-dimensional (0D) nanomaterials, such as quantum dots[63], inorganic nanoparticles[64] and polymeric nanoparticles[65], have been explored for similar biomedical applications. Polymeric nanoparticles have high biocompatibility, are easily functionalized, and their composition and structure can be tailored for specific applications[66]; for example, polydopamine nanoparticles (PDA-NPs) can be employed as biocompatible and biodegradable optical nano-transducers due to their photothermal response[67].

The optical properties and downstream energy conversion of one-dimensional (1D) nanomaterials, such as nanorods and nanowires, can be tailored by altering their chemical composition and physical properties[68,69]. Semiconductor nanowires, such as SiNWs, have been implemented in various biointerfaces to record and manipulate cellular and tissue electrophysiology[7,70,71]. SiNWs can be produced and customized using bottom-up synthesis processes, allowing the design of a variety of features, including diameter, length, dopant type (p-type or n-type) and doping ratio[72,73]. Coaxial p-i-n SiNWs exhibit photoelectric properties[74], whereas polycrystalline SiNWs have photothermal properties[37]. Furthermore, decorating SiNWs with AuNPs through controlled diffusion of an Au catalyst creates hybrid structures that combine the properties of both SiNWs and AuNPs[31].

2D nanomaterials, such as graphene, black phosphorous (single layer of P atoms), transition metal dichalcogenides, and transition metal carbides and nitrides (MXenes, transition metals sandwiched between 2D flakes of carbon or nitrogen atoms[75–77]), are being explored for various biomedical applications, including photothermal therapy, photodynamic therapy and photothermal modulation[78]. The library of 2D materials for biomedical applications is rapidly growing; for example, a large number of MXenes have been developed by altering their atomic composition and surface terminations[75–77]. For instance, titanium carbide ($Ti_3C_2T_x$, where T_x indicates the surface termination functional group, for example, -O, -OH or -F)[75,76] has been widely explored for biomedical and photothermal applications[75,76,79–81] due to its high electrical conductivity, high near-infrared (NIR) absorbance and high photothermal energy conversion efficiency[82]. High absorption in the NIR window is crucial for in vivo applications since, compared to visible wavelengths, NIR has reduced absorption by water and haemoglobin, allowing greater penetration depths in tissues[83]. Furthermore, the large-scale production of MXenes allows biointerfaces across multiple scales with individual flakes or films[40,84].

Three-dimensional (3D) and hybrid nanomaterials are an emerging class of nanomaterials for biomedical applications due to their exceptionally high and exposed surface area, electrochemical properties, and ability to form tight interfaces with cells[85]. Nanowire-templated 3D fuzzy graphene (NT-3DFG) is a hybrid nanomaterial composed of free-standing, single-to-few-layer graphene flakes directly synthesized on SiNWs through a bottom-up chemical vapour deposition synthesis protocol[29,86–90]. The 3D arrangement of vertically standing graphene flakes results in a high surface area[86], high number of active sites[88], high optical absorbance and photothermal conversion efficiency, and easy surface modification[29]. Such graphene nanostructures hold potential as input–output biointerfaces owing to precise control over the material structure and properties[9,85,86].

Photothermal energy conversion—Photothermal nanomaterials for biomedical applications should exhibit high optical absorbance and high optical-to-thermal energy conversion. The optical properties of metal nanoparticles, in particular, AuNPs and Au nanorods (AuNRs), depend on the wavelength of the incident light[91]. The oscillating electromagnetic field of the incident light induces coherent oscillations of the free electrons in Au[92,93]. The frequency of maximum amplitude of these oscillations is defined as surface plasmon resonance (SPR)[93], which is responsible for a strong wavelength-dependent optical absorption[91]. The intensity and wavelength of the SPR band depend on factors influencing the electron density of the nanoparticle surface such as particle size, shape and microstructure[92,93]. Increasing the size of AuNPs generally leads to an increase in the wavelength and intensity of the optical absorption peak[94]. Changing the shape of AuNPs to AuNRs splits the optical absorption into bands: longitudinal (a band of high intensity in the NIR region) and transverse (a band of low intensity in the visible region)[91]. The longitudinal band undergoes a redshift with an increase in the aspect ratio of the AuNRs[91,95,96]. Similar to AuNPs and AuNRs, $Ti_3C_2T_x$ also exhibits SPR[40]. The inter-band electronic transitions to the vacant energy states of the functional groups in $Ti_3C_2T_x$ flakes lead to enhanced NIR absorption[40]. The wavelength of the optical absorption peak of $Ti_3C_2T_x$ is independent of flake size but is dependent on the surface functional groups, including type and ratio. Controlling the synthesis protocols of $Ti_3C_2T_x$ allows tuning of its surface chemistry and thus of its optical properties[97,98].

Wavelength-dependent optical absorption facilitates photothermal modulation with high specificity as well as multiplexing[39,91]; however, broadband optical absorption provides flexibility over the irradiation wavelength that can be used for photothermal modulation and therapy[29,37]. Nanostructuring of Si-based and C-based metamaterials increases the optical path of incident light through the material, resulting in light trapping-mediated enhancement of optical absorption[99–101]. A similar effect is observed in NT-3DFG nanostructures[29,102], where increasing the size and density of graphene flakes results in higher broadband absorption across the UV-NIR regime[29].

The local temperature increase triggered by photothermally active nanomaterials can be characterized using micropipette-based and nanopipette-based thermometry[29,31,37,39,40,103]. Here, the changes in local temperature are recorded as changes in the resistance of the micropipette/nanopipette proximal to the target nanoparticle during illuminating light pulses[29,104]. A temperature increase of ~1.5 K can be achieved by illuminating 20 nm

AuNPs with a laser pulse (532 nm, 1 ms, 31 J cm^{-2} per pulse)[39]. The local temperature can be further increased to ~9 K by increasing AuNPs concentration[39]. Aggregation of AuNRs and AuNPs can be prevented by silica coating, which does not interfere with their photothermal properties[103]. Irradiating silica-coated AuNRs with 1 ms laser pulses (780 nm, 170 J cm^{-2} per pulse) leads to a local temperature increase of ~3.5 K, and lengthening the pulse duration further increases the temperature[103].

Si-based semiconducting nanomaterials respond to incident optical radiation differently than Au-based nanomaterials[105,106]. Photons absorbed by the Si lattice lead to the separation of charge carriers[105,106]. Non-radiative recombination of these generated carriers converts the energy of the incident photons to thermal energy[37,105,106]. Intrinsic SiNWs (i-SiNWs) illuminated with a laser of 240 kW cm^{-2} (532 nm, 10 ms) can increase the local temperature by ~5.4 K (ref. [37]). Texturing and decorating i-SiNWs with AuNPs can improve their photothermal response by increasing surface area and roughness[31,107]. Alternatively, the overall optical absorption can be further increased by synthesizing hybrid nanomaterials and metamaterials that enable light trapping[108,109], resulting in subsequent improvement of the photothermal response as reported for NT-3DFG[29]. The extinction magnitude of individual NT-3DFG is greater than that of i-SiNWs due to the presence of free-standing graphene flakes; therefore, the overall photothermal effect is also greater[29]. The local temperature increase for NT-3DFG under a 1 ms laser pulse (635 nm, 3 J cm^{-2} per pulse) is up to ~6 K, which is 260-fold greater than that for i-SiNWs under similar conditions[29].

NIR-responsive $Ti_3C_2T_x$, in the form of macroscale suspensions, has high photothermal energy conversion properties[80,110]. Single $Ti_3C_2T_x$ flakes also exhibit exceptional photothermal properties with a local temperature increase of ~2.3 K and ~3.3 K under 635 nm and 808 nm laser pulses (1 ms, 3 J cm^{-2} per pulse), respectively[40]. $Ti_3C_2T_x$ in the form of thin films results in a local temperature increase of ~10.7 K under laser irradiation (635 nm, 1 ms, 3 J cm^{-2} per pulse)[40]. MXenes and hybrid nanomaterials, such as NT-3DFG and Au-decorated SiNWs, have high photothermal efficiencies with similar or greater local temperature increases using lower laser power densities[29,31,37,39,40,103] (Table 1).

Multi-scale biointerfaces with nanomaterials—The close interface between photothermally active nanomaterials and biological entities allows efficient heat transfer for subsequent photothermal modulation[40]. Engineering nanomaterial dimensions allows the tailoring of biointerfaces to match the versatile morphology of cells and tissues; for example, interactions between biological entities with AuNPs and AuNRs are generally non-cytotoxic, specifically to neuronal cells[111,112]. Such biointerfaces can be established by adding AuNP and AuNR suspensions to in vitro cell cultures; however, the interface between AuNPs and target neurons is weak and active perfusion of media results in rapid wash-out[39]. Conjugating antibodies, such as synthetic Ts1 (a neurotoxin from *Tityus serrulatus* that binds to voltage-gated Na^+ channels), to AuNPs increases their adhesion to cell membranes, creating stable biointerfaces[39]. On the other hand, 1D nanomaterials, such as SiNWs, are either endocytosed[111–113] or adhere to the cell membrane based on their dimensions and surface functionalization[31]. In the case of NT-3DFG, the surface chemistry of the out-of-plane graphene flakes can be modified with the $(KF)_4$ polypeptide to promote adherence to the cell membrane of dorsal root ganglion (DRG) neurons instead

of internalization[29] (Fig. 2a). Similarly, $Ti_3C_2T_X$ flakes and films can form an interface with DRG neurons without being internalized, and DRG neurons cultured on top of $Ti_3C_2T_X$ films adhere to the film without delamination[40] (Fig. 2b). Delivery of photothermally active nanomaterials in vivo can be achieved by direct injection of suspensions at the target site. AuNRs injected as a suspension into the sciatic nerve in rats led to their accumulation close to the plasma membrane of axons[111–113] (Fig. 2c).

Cytotoxicity and photothermal toxicity—The toxicity of nanomaterials and of the photothermal modulation process needs to be minimal to enable biological applications. Toxicity is affected by the cytotoxicity of nanomaterials[114], phototoxicity induced by light[115–117] and potential damage caused by hyperthermia[118].

The cytotoxicity of nanomaterials is dependent on their chemical composition and physical size. Cytotoxicity can be evaluated in vitro and in vivo by assessing cellular viability, mitochondrial activity, oxidative stress, integrity of the cell membrane, tissue inflammation and genotoxicity[114]. Nanocarbons, such as three-dimensional fuzzy graphene (3DFG), do not negatively affect cellular viability nor induce cellular stress in neurons and cardiac cells[9,119]. However, the effect of nanomaterials on cell viability is dependent on concentration; for example, an NT-3DFG concentration of 0.15 ± 0.01 μg ml^{-1} does not negatively affect DRG neuron viability, yet increasing the concentration to 0.75 ± 0.05 μg ml^{-1} decreases cellular viability[29]. Other nanomaterials, such as graphene nanoribbons and graphene oxide nanoparticles, show a similar correlation between concentration and viability[120,121]. The absence of cytotoxicity of $Ti_3C_2T_X$ has been reported in vitro for cell cultures, such as DRG neurons[40] and epithelial cells[122], as well as in vivo (mouse model)[123].

Excessive and prolonged light illumination can potentially damage the cell membrane, induce an apoptotic response or lead to the generation of toxic products[115–117]. The effect of light on cell structure and functions can be quantified by immunoblotting (for example, using the apoptotic marker annexin V) or fluorescence indicators (for example, labelling intracellular Ca^{2+})[117]. During illumination, redox reactions due to the photogenerated charge carriers on the surface of the nanomaterials can lead to the formation of reactive oxygen species (ROS)[124]. Increased quantities of ROS can oxidize cellular proteins, thereby disrupting cellular reduction and oxidation homeostasis[125,126].

Hyperthermia in photothermal modulation can cause damage to the nervous system, including vascular changes, direct neuronal damage, and functional and metabolic effects[127–129]. Cumulative equivalent minutes at 43 °C (CEM_{43}) is an accepted criterion for thermal dose assessment to evaluate thermal damage in tissues[128,129]. This parameter is defined as:

$$CEM_{43} = \Delta t * R_{\text{hyperthermia}}^{43-T}$$

where Δt is the summation over the length of exposure, T is the average temperature and $R_{\text{hyperthermia}}$ is a constant ($R_{\text{hyperthermia}} = 0.25$ for $T < 43$ °C and $R_{\text{hyperthermia}} = 0.5$ for $T < 43$ °C)[128]. Prolonged heating of the brain (for 4 h at 38 °C) causes irreversible cellular abnormalities

in the thalamus[130], inhibition of neural activity[131] and a decrease in metabolic activities[130] in rats. However, the effect of short-duration transient photothermal pulses (with a duration of ~1 ms or less) remains to be evaluated. Phototoxicity is highly dependent on the type of interface (internalization or attachment), light conditions and cell type[132]. Evaluation of the phototoxicity of nanomaterials in vitro and in vivo requires multiple assays, including cell viability, cell stress, apoptosis and generation of side species such as ROS. While ROS generation from AuNRs under different laser powers (530 nm, 200 ms, 25 and 51 mJ cm^{-2}) causes complex stress responses in neural cell cultures[132], lipid-coated PDA-NPs effectively scavenged ROS, preventing ROS-induced mitochondrial dysfunction[133]. The integrity of the cell plasma membrane with light pulses can be investigated using live-cell labelling; in the case of NT-3DFG, cellular fluorescence intensity is not altered upon irradiation with 635 nm and 1 ms laser pulses with different powers (1–10 Hz) for 10 s (ref. [29]). However, intense laser exposure (22 mW, 1 ms, 500 Hz for 5 s) causes immediate loss of cellular fluorescence[29].

Illuminating AuNRs in rat sciatic nerves does not cause pathologic abnormalities in histological sections under mild illumination conditions (980 nm, 1 ms, 0.956 J cm^{-2} per pulse)[113]. By contrast, high energy pulse illumination of AuNRs (2.23 J cm^{-2}) leads to irreversible physiological damage and loss of tissue integrity[113]. These findings provide valuable information regarding the effect of photothermal modulation on cytotoxicity and highlight that illumination conditions need to be optimized for each nanomaterial and target biointerface. Nevertheless, more comprehensive studies are required to determine safe operating conditions in vitro and in vivo.

Photothermal neural modulation

Photothermal neural excitation requires a rapid increase in localized temperature to alter the cell membrane capacitance and induce a depolarizing current[39,43]. Once the induced depolarizing current is greater than the cellular electrical threshold, any additional incident optical energy does not contribute significantly to further electrophysiological excitation[29]. Therefore, efficient photothermal excitation can be experimentally achieved through short laser pulses, generally with a pulse width of ~1 ms or lower, directed at the cell membrane and nanomaterial interface[29,31,39,40,42,134].

Photothermal inhibition of neural activity can also be achieved through a substantial and prolonged localized increase in temperature at the cell membrane, which alters membrane resistance[50,52]. Prolonged illumination of the nanomaterial–cell membrane interface (pulse width generally >100 ms) leads to the generation of transmembrane currents necessary for hyperpolarization[50]. Therefore, altering the light illumination conditions (pulse width, power density and spot size) allows seamless switching between neural excitation and inhibition[67,135–139].

High spatiotemporal stimulation and on-demand inhibition of neural activity in vitro (2D cell cultures, 3D spheroids and organoids) and in vivo will directly expand the understanding of network propagation of electrical currents across multiple dimensions.

Photothermal excitation of neural activity—Plasmonic particles, such as AuNPs and AuNRs, have been extensively used for photothermal excitation[39,103,134,140–143]. Stimulating AuNP-functionalized DRG neurons with either electrical (current pulses of 300 pA, 1 ms) or optical (light pulses of 532 nm, 1 ms, 31 J cm^{-2} per pulse) stimuli results in similar action potentials[39]. The increase in local temperature (~1.5 K) near the neuronal membrane during light pulses indicates that optical stimuli induce photothermal excitation[39]. The surface functionalization of AuNPs, such as through cholesterol conjugation[134], silica coating[103], polymer modifications (for example, cationized form of-high-density lipoprotein)[143] and antibody modifications (for example, anti-haemagglutinin and anti-thymocyte antigen 1)[140–142], can stabilize the binding and interfacing of AuNPs with the neuronal membrane and increase excitation efficiency. Such AuNPs have been used to stimulate multiple types of neurons, including rat primary auditory neurons (silica-coated AuNRs; 780 nm, 1 ms, 0.159 J cm^{-2} per pulse)[113], mice cortical neurons (AuNPs; 532 nm, 40 ms, 25 J cm^{-2} per pulse)[132], and NG108–15 mouse neuroblastoma and rat glioma hybrid cell lines (AuNRs; 785 nm, 100 ms, 0.33 J cm^{-2} per pulse)[144].

Broadband absorbers, such as Si-based and C-based nanomaterials, have also been explored for photothermal excitation[29,31,37]. SiNWs periodically patterned with AuNPs lead to Ca^{2+} transients in glial cell protrusion after laser illumination (592 nm, 1 ms, 113 J cm^{-2} per pulse) on the interface between SiNWs and the cells[31]. Ca^{2+} is an essential secondary indicator with a versatile signalling role in neural activation[145]. When a neuron elicits an action potential, Ca^{2+} ions enter the cell and depolarize the cell membrane[145]. The intracellular Ca^{2+} influx inside the cell suggests a subcellular resolution of excitation[31]. Mesoporous Si particles grown on an ordered hexagonal silica template also show a high photothermal response (~5.8 K local temperature increase with laser irradiation of 532 nm, 2.2 ms, 14.3 J cm^{-2} per pulse)[146]. An action potential can be generated in DRG neurons with a threshold energy of 5.32 μJ with a single mesoporous Si particle (532 nm, 1 ms, 6.8 J cm^{-2} per pulse)[146].

C-based nanomaterials are safe to use for photothermal activation, and their structures and properties can be easily tuned[9,42,85,147]; for example, graphite particles and carbon nanotubes can stimulate DRG neurons with multiple incident wavelengths (405 nm and 532 nm for graphite particles; 405 nm and 785 nm for carbon nanotubes) with a micro-joule (less than 5 μJ) energy per pulse[42]. Carbon nanohorns (CNHs) functionalized with NIR-excited dye (IRDye800CW) (dye-CNHs) have enhanced NIR absorption and increased photothermal conversion of the incident optical energy[147]. Illuminating DRG neurons interfaced with dye-CNHs (800 nm laser illumination for 300 s) results in an increased intracellular Ca^{2+} fluorescence intensity, where the Ca^{2+} influx indicates the depolarization of the cell membrane[145,147]. The excitation mechanism was proposed to be the activation of temperature-sensitive ion channels[147]. Photothermal excitation with NT-3DFG is highly reproducible and can be used to activate target neurons at various laser pulse frequencies (1 Hz, 10 Hz and 20 Hz pulses)[27]. The patch-clamp technique allows direct recordings of membrane potential and currents[148]. Both patch-clamp and real-time Ca^{2+} fluorescence imaging can be applied to record electrical activity induced upon photothermal stimulation of DRG neurons at a single-cell and network level, respectively[29] (Fig. 3a). By altering

the incident energy per pulse, NT-3DFG achieves sub-threshold (~2.73 μJ per pulse) or complete cellular activation (~3.62 μJ per pulse)[29] (Fig. 3b). Beyond 2D cell cultures, cortical neural spheroids can be photothermally excited by interfacing with NT-3DFG, demonstrating modulation of the electrical activity of 3D cellular networks[29].

2D nanoflakes have also been used for photothermal modulation of cellular activity[40,149]. Polyethylene glycol (PEG)-modified black phosphorus nanoflakes can modulate the electrical activity of hippocampal neurons (808 nm, 30 ms, 0.06 J cm^{-2} per pulse)[149]. Activation of electrical activity across a network of DRG neurons was also achieved by interfacing with $Ti_3C_2T_x$ films and flakes, resulting in intracellular Ca^{2+} transients following illumination with single light pulses (532 nm, 1 ms, 0.6 and 5.7 J cm^{-2} per pulse for films and flakes, respectively)[40] (Fig. 3c).

Engineered organic nanostructures have enabled NIR photothermal excitation[41,133]. Semiconducting polymer nano-bioconjugates (SPNs) have absorption peaks in the NIR window (~800 nm) and higher photothermal conversion efficiency compared to AuNRs[41]. Here, the NIR response of SPNs is a result of specific alterations of the chemical composition of the semiconducting polymers, for example, poly(cyclopentadithiophene-alt-diketopyrrolopyrrole) and poly(cyclopentadithiophene-alt-benzothiadiazole)[41]. TRPV1-expressing mouse neuroblastoma cells (ND7/23) in the presence of SPNs (poly(cyclopentadithiophene-alt-benzothiadiazole)) show Ca^{2+} transient oscillations that correlate with the applied laser pulses (808 nm laser with 0.5 s switching on and off intervals)[41]. Illuminating $TRPV1^-$ cells does not result in similar Ca^{2+} transients, suggesting a neural activation mechanism by temperature-sensitive ion channels[41]. Using lipid-coated PDA-NPs labelled with a temperature-sensitive dye (ER Thermo Yellow) result in a ~2.69 K temperature increase with laser irradiation (808 nm, 8,496 J cm^{-2}) and an increase in Ca^{2+} intensity for 60 s (ref. [133]).

The illumination conditions for photothermal excitation need to be optimized for different types of photothermally active nanomaterials and neurons (Supplementary table 1). Nanomaterials that lead to high temperature increases, such as NT-3DFG, black phosphorus nanoflakes and $Ti_3C_2T_x$ MXene films, require lower energies to achieve successful photothermal excitation compared to AuNPs and SiNWs[29,40]. A lower incident energy is preferred to minimize potential damage to light-targeted cells and tissues. This property should be considered in the design of photothermal materials for neural modulation.

Owing to the limited penetration depth of visible light in tissues, it is important to improve the photothermal performance of nanomaterials in biological transparency windows, including NIR-I (700–900 nm) and NIR-II (1,000–1,700 nm)[150,151]. Scattering and absorption of light in tissues contribute to the attenuation of light intensity as a function of depth, thereby limiting the efficiency of incident light pulses for optical modulation[150,151]. The scattering of incident light is attributed to the inhomogeneity of refractive indices of different components inside tissues[151,152] and is inversely proportional to the wavelength according to Mie and Rayleigh scattering principles[153,154]. Absorption of incident light is attributed to the presence of water, lipids and biomolecules, for example, chromophores, such as haeme, that exist in haemoglobin[150,151]. The restrictions

on wavelengths of illuminating light pulses limit the selection of nanomaterials for in vivo photothermal modulation in the peripheral nervous system (PNS) and the central nervous system (CNS)[41,53,113,142,147,149]. Sciatic nerve (PNS) action potential can be induced by injecting AuNRs proximal to the nerve and illuminating the interface (980 nm, 1 ms, 0.64 J cm^{-2} per pulse)[113]. The electrophysiology of the nerve can then be recorded with W electrodes at the distal end[113]. Injection of AuNRs and direct infrared illumination results in a three-fold lower excitation threshold compared with illumination without AuNRs (0.159 and 0.480 J cm^{-2} per pulse with and without AuNRs, respectively)[113]. Nanomaterial-assisted photothermal modulation can also be employed to regulate muscle activity[41,147]; for example, dye-functionalized CNHs injected under the thigh of a euthanized frog elicit paw twitch following light illumination (800 nm, continuous wave illumination, 292 mW mm^{-2})[41,147] whereas no twitches are observed in the absence of CNHs under the same light illumination condition[41,147].

Injecting PEG-modified black phosphorus nanoflakes into the visual cortex (CNS) of a rat enables the simultaneous monitoring of neural activity using W microelectrodes[149] (Fig. 3d). Here, upon NIR illumination (808 nm, 50 ms, 0.15 J cm^{-2} per pulse), the amplitude of the evoked action potential increases[149] (Fig. 3d). AuNRs injected in the whisker-controlling region of a rat's motor cortex result in whisker oscillation following NIR illumination (980 nm, 2 s pulse (300 Hz, 1.5 ms duration), 0.128 J cm^{-2} per pulse), whereas no significant oscillations are observed with only light illumination and absence of AuNRs[142]. However, induced movement of the whisker triggered by photothermal excitation using AuNRs is short and slow compared to that induced using electrical stimuli (amplitude of 2.4 mA, 300 Hz, 0.2 ms pulse duration)[142]. Deep brain neuromodulation was demonstrated in freely moving mice using macromolecular NIR-II-absorbing polymeric nanoparticles (MINDS). These core–shell structured particles were composed of a core of poly(benzobisthiadiazole-alt-vinylene) and a shell of poly(lactide-co-glycolide)-*b*-poly(ethylene glycol)), with an absorption peak at 1,046 nm, engineered by adjusting the molecular orbitals of the donor and acceptor units in the particles[53]. However, this platform requires genetic modification for TRPV1 expression in target neurons and heating of neural tissues for TRPV1 activation, resulting in slow response times (~seconds) and limiting clinical translation[53]. Therefore, further work is needed to improve the robustness and efficiency of nanomaterial-facilitated non-genetic photothermal excitation.

Photothermal inhibition of neural activity—Photothermal agents enable the suppression of neural activity with cellular-scale resolution without irreversible physiological damage to cells and tissues[1,54,136]. Reversible and non-genetic inhibition of neural activity is valuable for the understanding of brain functions and for pain management[136].

Various forms of Au-based nanoparticles allow photothermal inhibition of neural activity[54,136,137,155,156]; for example, AuNRs can be interfaced with hippocampal neurons and illuminated with a 785 nm pulsed laser (10 s light on and 20 s light off)[136] (Fig. 4a,b). Upon illumination at 15 J cm^{-2}, neuron firing events are suppressed owing to an increase in temperature of ~5 K under 10 s light illumination[136] (Fig. 4a). Removing pulsed illumination restores the original neuronal state[136]. As the laser power increases from 0 to

15 mW mm^{-2} (15 J cm^{-2}), the percentage of suppression also monotonically increases from 0 to 89.6%[136] (Fig. 4b) owing to the activation of the TREK1 channel (thermosensitive K^+ channel)[136]. Instead of dispersing AuNPs randomly in cell cultures, patterning AuNRs using inkjet printing[138] and incident light patterning using a digital micromirror[137] facilitates spatial control of individual neurons activity suppression at the patterned sites.

Polymer particles, such as PDA-NPs, can also inhibit neural activity[67], depending on laser power and duration[67]. Increasing the laser power density from 3 to 6 mW mm^{-2} (with illumination for 10, 20 or 30 s) or increasing the pulse duration from 5 to 45 s (with 3, 4 or 6 mW mm^{-2}) results in greater cell hyperpolarization[67]. This leads to longer delays in the recovery of spontaneous electrical activity of the target neurons post-termination of illumination[67]. Firing of primary hippocampal neurons (change in spontaneous activity) cultured on a poly(3-hexylthiophene) (P3HT) film is inhibited following laser illumination with shorter pulse duration (540 nm, 1 s, 16 mW mm^{-2})[139]. By contrast, the inhibition efficiency of spontaneous neural activity does not change by adding a TRPV blocker (Ruthenium Red). This result suggests that the hyperpolarization of the cell membrane is independent of TRPV, and is likely related to the change of membrane-resistive elements[139]. A blended semiconductor polymer (P3HT:phenyl-C61-butyric acid methyl ester) allows spatial-selective photothermal inhibition of activity in explanted peripheral nerves by changing the position of the light spot along the nerve[54]. Hybrid film structures, such as graphene-conjugated and poly(3,4-ethylenedioxythiophene)-poly(styrenesulfonate)-conjugated P3HT films, can increase photothermal conversion performance[135]. The higher local heat generated by the graphene-conjugated P3HT structure (compared to poly(3,4-ethylenedioxythiophene)-poly(styrenesulfonate)-conjugated P3HT film) enables light-induced firing modulation in primary hippocampal neurons (550 nm, 500 ms, 0.75 J cm^{-2})[135]. Conjugation with graphene enables more efficient separation of charges generated under illumination in the neighbouring P3HT molecules due to work-function matching[135]. Preliminary ex vivo validation in blind retina explants extracted from rat demonstrated that the graphene-conjugated P3HT structure improves the activity of retinal ganglion cells, and may thus provide a viable tool for neural activity modulation[135].

Photothermal modulation of signalling pathways and physiology—Photothermal techniques can be applied to modulate signalling pathways and regulate cellular physiology for therapeutic interventions, for example, for drug delivery and nerve regeneration[44,45,157,158]. AuNRs functionalized with thiol-modified oligonucleotides allow remote and selective control of nucleotide release within neural cells under illumination with a 785 nm laser[157]. Similarly, conjugating DNA on AuNRs with different absorption peaks can achieve selective DNA release under different wavelengths of illumination[158]. 2D MoS_2, a type of transition metal dichalcogenide, exhibits high photothermal response at the NIR wavelength and can modulate the expression of 157 genes in human mesenchymal stem cells under light illumination (800 nm, 7 min, 0.14 J cm^{-2}) to regulate cellular migration, integrin signalling and wound healing[159]. Importantly, MoS_2 and NIR treatment do not activate stress-related pathways in human mesenchymal stem cells[159].

Damaged nerve tissue could be regenerated by photothermal modulation, for example, by accelerating neural growth and differentiation of neural stem cells into neurons[160].

Illumination of neural stem cells seeded on Au nanocage-coated extracellular matrix (808 nm, 1 min, 120 J cm^{-2}) increased neuronal differentiation of rat fetal neural stem cells from 27.9% to 56.0% due to the thermal activation of the heat shock protein pathway[44]. Additionally, illuminating NG108–15 cells (mouse neuroblastoma and rat glioma hybrid cell lines) cultured with AuNRs with NIR light (780 nm, 1 min, 450 J cm^{-2}) results in 36% longer neurite growth compared to cells incubated with AuNRs without laser illumination, which may be attributed to activation of transcription factors that promote cell metabolic activity[45].

Developing nanomaterials with a multifaceted optical response is a potential approach for efficient modulation of cellular physiology and signalling pathways; for example, photothermal and photoelectric responses of P3HT films can increase cellular proliferation and tubulogenesis of endothelial colony-forming cells through the activation of TRPV1 ion channels[161]. In addition, the photoelectric response of P3HT regulates neuronal growth and cellular signalling pathways such as redox signalling due to cytochrome c protein[162,163].

Outlook

Engineering the chemical composition, size and structure of photothermally active nanomaterials provides control over material properties and enables versatile multi-scale biointerfaces with individual neural cells, engineered neural tissues and animal models. In addition, cellular activity can be controlled by tailoring the parameters of the input optical pulses. Photothermal modulation has a high potential for extended applications in both in vitro and in vivo systems with synergistic multidisciplinary developments.

Modulating 3D in vitro systems—Engineered 3D tissues are promising models for drug discovery and personalized medicine[164]. Such tissue models can be fabricated by 3D bioprinting, which offers precise control over tissue architecture and microenvironment[165]; for example, cortical spheroids are powerful models for the investigation of tissue development, disease progression and pharmacological drug testing[166]. Embedding photothermally active nanomaterials in nodes distributed throughout engineered 3D tissues can provide precise spatiotemporal control over their electrophysiology. Coupled with fluorescence imaging, recording and sensing technologies, this technique will enable 3D tracking of neural networks and signal propagation[29].

Photothermally active nanomaterials embedded in artificial 3D tissue constructs also allow direct modulation of biochemical signalling pathways and transcription of target proteins with high spatiotemporal resolution; for example, coupling photothermal agents with temperature-sensitive proteins, such as heat shock proteins inside the cytoplasm, may facilitate spatial and temporal control of gene expression through photothermal effects[167,168]. Combining tissue engineering approaches with photothermal modulation will help to study and control cellular processes and functions with subcellular resolution.

In vivo therapeutics—Remote and non-genetic modulation of neural activity makes photothermal modulation an attractive alternative as neural therapeutics. Optical neuromodulation requires minimally invasive input and output interfaces between neurons and photothermal agents; for example, photothermally active nanomaterials can be

accurately injected at identified seizure foci through a minimally invasive procedure for targeted photothermal neural excitation or inhibition. By contrast, conventional neuromodulation approaches rely on deep brain stimulation and responsive neurostimulation to target seizure foci, which requires invasive surgeries and macroscopic implants[48,169].

Optogenetic therapeutics have successfully rescued motor and behavioural functions in mice with Parkinson disease[47]. Photothermal modulation is a non-genetic alternative to such approaches. In particular, photocatalytic mechanisms can be exploited to localize and control the synthesis of signalling molecules regulating cellular signalling pathways[170,171]. Such mechanisms can also be leveraged for photothermal activation to generate small molecules at the cellular and tissue levels, for example, in situ photoelectrochemical synthesis of H_2O_2 for the regulation of smooth muscle contraction via an inositol triphosphate receptor-based mechanism[170–172].

Photothermal modulation has been demonstrated in rodents by either injecting nanomaterials or implanting patterned thin films close to the target tissues[53,113,142,149]. Translation of photothermal modulation techniques into non-human primates has not been reported. Photothermal modulation has a high possibility of translation to clinical trials given the ease of employing for both the CNS and PNS[53,113,142,149]. However, the clinical translation of photothermally active nanomaterials necessitates further technological developments, including cell-specific control, localized delivery of light pulses and engineering of biointerface stability (Box 2). The regulatory protocols for clinical translation should require detailed evaluation of the safety and efficacy of the technique as well as the cytotoxicity and phototoxicity of nanomaterials in acute and chronic applications.

Citation diversity statement

We acknowledge that papers authored by scholars from historically excluded groups are systematically under-cited. Here, we have made every attempt to reference relevant papers in a manner that is equitable in terms of racial, ethnic, gender and geographical representation.

Supplementary Material

Refer to Web version on PubMed Central for supplementary material.

Acknowledgements

T.C.-K. acknowledges funding support from the Defense Advanced Research Projects Agency (Award No. D20AC00002) and the National Institute of Health (Award No. R21EB029164).

References

1. Liang E, Shi J. & Tian B. Freestanding nanomaterials for subcellular neuronal interfaces. iScience 25, 103534 (2022). [PubMed: 34977499]
2. Hong J.-w, Yoon C, Jo K, Won JH & Park S. Recent advances in recording and modulation technologies for next-generation neural interfaces. iScience 24, 103550 (2021). [PubMed: 34917907]
3. Kang S-K, Koo J, Lee YK & Rogers JA Advanced materials and devices for bioresorbable electronics. Acc. Chem. Res 51, 988–998 (2018). [PubMed: 29664613]

4. Rogers JA, Someya T. & Huang Y. Materials and mechanics for stretchable electronics. Science 327, 1603–1607 (2010). [PubMed: 20339064]
5. Song E, Li J, Won SM, Bai W. & Rogers JA Materials for flexible bioelectronic systems as chronic neural interfaces. Nat. Mater 19, 590–603 (2020). [PubMed: 32461684]
6. Hong G. & Lieber CM Novel electrode technologies for neural recordings. Nat. Rev. Neurosci 20, 330–345 (2019). [PubMed: 30833706]
7. Zhang A. & Lieber CM Nano-bioelectronics. Chem. Rev 116, 215–257 (2016). [PubMed: 26691648]
8. Balakrishnan G, Song J, Mou C. & Bettinger CJ Recent progress in materials chemistry to advance flexible bioelectronics in medicine. Adv. Mater 34, 2106787 (2022).
9. Garg R, Roman DS, Wang Y, Cohen-Karni D. & Cohen-Karni T. Graphene nanostructures for input–output bioelectronics. Biophys. Rev 2, 041304 (2021).
10. Bergman H, Wichmann T. & DeLong MR Reversal of experimental parkinsonism by lesions of the subthalamic nucleus. Science 249, 1436–1438 (1990). [PubMed: 2402638]
11. Spira ME & Hai A. Multi-electrode array technologies for neuroscience and cardiology. Nat. Nanotechnol 8, 83–94 (2013). [PubMed: 23380931]
12. Engel AK, Moll CK, Fried I. & Ojemann GA Invasive recordings from the human brain: clinical insights and beyond. Nat. Rev. Neurosci 6, 35–47 (2005). [PubMed: 15611725]
13. Polikov VS, Tresco PA & Reichert WM Response of brain tissue to chronically implanted neural electrodes. J. Neurosci. Methods 148, 1–18 (2005). [PubMed: 16198003]
14. Rivnay J, Wang H, Fenno L, Deisseroth K. & Malliaras GG Next-generation probes, particles, and proteins for neural interfacing. Sci. Adv 3, e1601649 (2017).
15. Gulino M, Kim D, Pané S, Santos SD & Pêgo AP Tissue response to neural implants: the use of model systems toward new design solutions of implantable microelectrodes. Front. Neurosci 13, 689 (2019). [PubMed: 31333407]
16. Carnicer-Lombarte A, Chen S-T, Malliaras GG & Barone DG Foreign body reaction to implanted biomaterials and its impact in nerve neuroprosthetics. Front. Bioeng. Biotechnol 9, 622524 (2021). [PubMed: 33937212]
17. Salatino JW, Ludwig KA, Kozai TD & Purcell EK Glial responses to implanted electrodes in the brain. Nat. Biomed. Eng 1, 862–877 (2017). [PubMed: 30505625]
18. Boyden ES, Zhang F, Bamberg E, Nagel G. & Deisseroth K. Millisecond-timescale, genetically targeted optical control of neural activity. Nat. Neurosci 8, 1263–1268 (2005). [PubMed: 16116447]
19. Sahel J-A et al. Partial recovery of visual function in a blind patient after optogenetic therapy. Nat. Med 27, 1223–1229 (2021). [PubMed: 34031601]
20. Chernov M. & Roe AW Infrared neural stimulation: a new stimulation tool for central nervous system applications. Neurophotonics 1, 011011 (2014). [PubMed: 26157967]
21. Packer AM, Roska B. & Häusser M. Targeting neurons and photons for optogenetics. Nat. Neurosci 16, 805–815 (2013). [PubMed: 23799473]
22. Plaksin M, Shapira E, Kimmel E. & Shoham S. Thermal transients excite neurons through universal intramembrane mechanoelectrical effects. Phys. Rev. X 8, 011043 (2018).
23. Wells J. et al. Optical stimulation of neural tissue in vivo. Opt. Lett 30, 504–506 (2005). [PubMed: 15789717]
24. Wells JD, Kao C, Jansen ED, Konrad PE & Mahadevan-Jansen A. Application of infrared light for in vivo neural stimulation. J. Biomed. Opt 10, 064003 (2005). [PubMed: 16409069]
25. Jenkins MW et al. Optical pacing of the embryonic heart. Nat. Photonics 4, 623–626 (2010). [PubMed: 21423854]
26. Liljemalm R, Nyberg T. & von Holst H. Heating during infrared neural stimulation. Lasers Surg. Med 45, 469–481 (2013). [PubMed: 23832680]
27. Wells JD et al. Optically mediated nerve stimulation: Identification of injury thresholds. Lasers Surg. Med 39, 513–526 (2007). [PubMed: 17659590]
28. Zimmerman JF & Tian B. Nongenetic optical methods for measuring and modulating neuronal response. ACS Nano 12, 4086–4095 (2018). [PubMed: 29727159]

29. Rastogi SK et al. Remote nongenetic optical modulation of neuronal activity using fuzzy graphene. Proc. Natl Acad. Sci. USA 117, 13339–13349 (2020). [PubMed: 32482882] This article reports templated graphene nanostructures that enable remote, non-genetic photothermal stimulation with laser energies as low as sub-hundred nanojoules without generating cellular stress.
30. Chen R, Romero G, Christiansen MG, Mohr A. & Anikeeva P. Wireless magnetothermal deep brain stimulation. Science 347, 1477–1480 (2015). [PubMed: 25765068]
31. Fang Y. et al. Texturing silicon nanowires for highly localized optical modulation of cellular dynamics. Nano Lett. 18, 4487–4492 (2018). [PubMed: 29894630]
32. Sebesta C. et al. Subsecond multichannel magnetic control of select neural circuits in freely moving flies. Nat. Mater 21, 951–958 (2022). [PubMed: 35761060]
33. Duret G. et al. Magnetic entropy as a proposed gating mechanism for magnetogenetic ion channels. Biophys. J 116, 454–468 (2019). [PubMed: 30665695]
34. Jiang Y. & Tian B. Inorganic semiconductor biointerfaces. Nat. Rev. Mater 3, 473–490 (2018). [PubMed: 31656635]
35. Ghezzi D. et al. A hybrid bioorganic interface for neuronal photoactivation. Nat. Commun 2, 166 (2011). [PubMed: 21266966] This article presents photothermal excitation of primary neurons using short pulses of visible light at the interfaced organic thin films.
36. Bareket-Keren L. & Hanein Y. Novel interfaces for light directed neuronal stimulation: advances and challenges. Int. J. Nanomed 9, 65 (2014).
37. Jiang Y. et al. Rational design of silicon structures for optically controlled multiscale biointerfaces. Nat. Biomed. Eng 2, 508–521 (2018). [PubMed: 30906646]
38. Ye E. & Li Z. Photothermal Nanomaterials. Vol. 54 (Royal Society of Chemistry, 2022).
39. Carvalho-de-Souza JL et al. Photosensitivity of neurons enabled by cell-targeted gold nanoparticles. Neuron 86, 207–217 (2015). [PubMed: 25772189]
40. Wang Y. et al. Ti3C2Tx MXene flakes for optical control of neuronal electrical activity. ACS Nano 15, 14662–14671 (2021). [PubMed: 34431659] The article reports 2D MXene films and flakes that enable subcellular photothermal stimulation with energies as low as tens of microjoules per pulse.
41. Lyu Y, Xie C, Chechetka SA, Miyako E. & Pu K. Semiconducting polymer nanobioconjugates for targeted photothermal activation of neurons. J. Am. Chem. Soc 138, 9049–9052 (2016). [PubMed: 27404507]
42. Carvalho-de-Souza JL, Pinto BI, Pepperberg DR & Bezanilla F. Optocapacitive generation of action potentials by microsecond laser pulses of nanojoule energy. Biophys. J 114, 283–288 (2018). [PubMed: 29273263]
43. Pinto BI, Bassetto CA & Bezanilla F. Optocapacitance: physical basis and its application. Biophys. Rev 14, 569–577 (2022). [PubMed: 35528029] This article explains the theoretical basis of optocapacitive-based photothermal excitation.
44. Jung S. et al. Photothermal response induced by nanocage-coated artificial extracellular matrix promotes neural stem cell differentiation. Nanomaterials 11, 1216 (2021). [PubMed: 34064443]
45. Paviolo C. et al. Laser exposure of gold nanorods can increase neuronal cell outgrowth. Biotechnol. Bioeng 110, 2277–2291 (2013). [PubMed: 23456616]
46. Masini D. & Kiehn O. Targeted activation of midbrain neurons restores locomotor function in mouse models of parkinsonism. Nat. Commun 13, 504 (2022). [PubMed: 35082287]
47. Zhang Y. et al. Targeting thalamic circuits rescues motor and mood deficits in PD mice. Nature 607, 321–329 (2022). [PubMed: 35676479]
48. Li MC & Cook MJ Deep brain stimulation for drug-resistant epilepsy. Epilepsia 59, 273–290 (2018). [PubMed: 29218702]
49. Hodgkin AL & Huxley AF A quantitative description of membrane current and its application to conduction and excitation in nerve. J. Physiol 117, 500–544 (1952). [PubMed: 12991237]
50. Manfredi G. et al. The physics of plasma membrane photostimulation. APL Mater. 9, 030901 (2021). This article describes the physical phenomena responsible for photostimulation using the simple equivalent circuit model of the cell membrane.
51. Eom K, Byun KM, Jun SB, Kim SJ & Lee J. Theoretical study on gold-nanorod-enhanced near-infrared neural stimulation. Biophys. J 115, 1481–1497 (2018). [PubMed: 30266321]

52. Martino N. et al. Photothermal cellular stimulation in functional bio-polymer interfaces. Sci. Rep 5, 8911 (2015). [PubMed: 25753132]
53. Wu X. et al. Tether-free photothermal deep-brain stimulation in freely behaving mice via wide-field illumination in the near-infrared-II window. Nat. Biomed. Eng 6, 754–770 (2022). [PubMed: 35314800] This article demonstrates in vivo photothermal stimulation of TRPV1-expressing neurons using NIR-II responsive macromolecular transductors.
54. Gribi S, du Bois de Dunilac S, Ghezzi D & Lacour SP A microfabricated nerve-on-a-chip platform for rapid assessment of neural conduction in explanted peripheral nerve fibers. Nat. Commun 9, 4403 (2018). [PubMed: 30353009]
55. Patapoutian A, Peier AM, Story GM & Viswanath V. ThermoTRP channels and beyond: mechanisms of temperature sensation. Nat. Rev. Neurosci 4, 529–539 (2003). [PubMed: 12838328]
56. Ramos AP, Cruz MA, Tovani CB & Ciancaglini P. Biomedical applications of nanotechnology. Biophys. Rev 9, 79–89 (2017). [PubMed: 28510082]
57. McNamara K. & Tofail SA Nanoparticles in biomedical applications. Adv. Phys X 2, 54–88 (2017).
58. Vajtai R. Springer Handbook of Nanomaterials (Springer Science & Business Media, 2013).
59. Wang Y. & Guo L. Nanomaterial-enabled neural stimulation. Front. Neurosci 10, 69 (2016). [PubMed: 27013938]
60. Dykman L. & Khlebtsov N. Gold nanoparticles in biology and medicine: recent advances and prospects. Acta Naturae 3, 34–55 (2011). [PubMed: 22649683]
61. Giljohann DA et al. In Spherical Nucleic Acids, 55–90 (Jenny Stanford Publishing, 2020).
62. Roper DK, Ahn W. & Hoepfner M. Microscale heat transfer transduced by surface plasmon resonant gold nanoparticles. J. Phys. Chem C. 111, 3636–3641 (2007).
63. Bera D, Qian L, Tseng T-K & Holloway PH Quantum dots and their multimodal applications: a review. Materials 3, 2260–2345 (2010).
64. Altavilla C. & Ciliberto E. Inorganic Nanoparticles: Synthesis, Applications, and Perspectives (CRC Press, 2017).
65. Rao JP & Geckeler KE Polymer nanoparticles: preparation techniques and size-control parameters. Prog. Polym. Sci 36, 887–913 (2011).
66. Zielińska A. et al. Polymeric nanoparticles: production, characterization, toxicology and ecotoxicology. Molecules 25, 3731 (2020). [PubMed: 32824172]
67. Gholami Derami H. et al. Reversible photothermal modulation of electrical activity of excitable cells using polydopamine nanoparticles. Adv. Mater 33, 2008809 (2021).
68. Yan R, Gargas D. & Yang P. Nanowire photonics. Nat. Photonics 3, 569–576 (2009).
69. Shi J, Sun C, Liang E. & Tian B. Semiconductor nanowire-based cellular and subcellular interfaces. Adv. Funct. Mater 32, 2107997 (2021).
70. Tian B. et al. Three-dimensional, flexible nanoscale field-effect transistors as localized bioprobes. Science 329, 830–834 (2010). [PubMed: 20705858]
71. Zhou W, Dai X. & Lieber CM Advances in nanowire bioelectronics. Rep. Prog. Phys 80, 016701 (2016). [PubMed: 27823988]
72. Wagner AR & Ellis SW Vapor-liquid-solid mechanism of single crystal growth. Appl. Phys. Lett 4, 89–90 (1964).
73. Schmidt V, Wittemann J. & Gosele U. Growth, thermodynamics, and electrical properties of silicon nanowires. Chem. Rev 110, 361–388 (2010). [PubMed: 20070117]
74. Tian B. et al. Coaxial silicon nanowires as solar cells and nanoelectronic power sources. Nature 449, 885–889 (2007). [PubMed: 17943126]
75. VahidMohammadi A, Rosen J. & Gogotsi Y. The world of two-dimensional carbides and nitrides (MXenes). Science 372, eabf1581 (2021).
76. Naguib M. et al. Two-dimensional nanocrystals produced by exfoliation of Ti3AlC2. Adv. Mater 23, 4248–4253 (2011). [PubMed: 21861270]
77. Gogotsi Y. & Huang Q. MXenes: two-dimensional building blocks for future materials and devices. ACS Nano 15, 5775–5780 (2021). [PubMed: 33906288]

78. Gao P. et al. Biomedical applications of 2D monoelemental materials formed by group VA and VIA: a concise review. J. Nanobiotechnol 19, 96 (2021).
79. Driscoll N. et al. Two-dimensional Ti3C2 MXene for high-resolution neural interfaces. ACS Nano 12, 10419–10429 (2018). [PubMed: 30207690]
80. Lin H, Wang X, Yu L, Chen Y. & Shi J. Two-dimensional ultrathin MXene ceramic nanosheets for photothermal conversion. Nano Lett. 17, 384–391 (2017). [PubMed: 28026960]
81. Driscoll N. et al. MXene-infused bioelectronic interfaces for multiscale electrophysiology and stimulation. Sci. Transl. Med 13, eabf8629 (2021).
82. Hantanasirisakul K. & Gogotsi Y. Electronic and optical properties of 2D transition metal carbides and nitrides (MXenes). Adv. Mater 30, 1804779 (2018).
83. Yaroslavsky AN et al. Optical properties of selected native and coagulated human brain tissues in vitro in the visible and near infrared spectral range. Phys. Med. Biol 47, 2059–2073 (2002). [PubMed: 12118601]
84. Shuck CE et al. Scalable synthesis of $Ti3C2T_x$ MXene. Adv. Eng. Mater 22, 1901241 (2020).
85. San Roman D, Garg R. & Cohen-Karni T. Bioelectronics with graphene nanostructures. APL Mater. 8, 100906 (2020).
86. Garg R. et al. Nanowire-mesh-templated growth of out-of-plane three-dimensional fuzzy graphene. ACS Nano 11, 6301–6311 (2017). [PubMed: 28549215]
87. Garg R. et al. Electron transport in multidimensional fuzzy graphene nanostructures. Nano Lett. 19, 5335–5339 (2019). [PubMed: 31265782]
88. San Roman D. et al. Engineering three-dimensional (3D) out-of-plane graphene edge sites for highly selective two-electron oxygen reduction electrocatalysis. ACS Catal. 10, 1993–2008 (2020).
89. Rastogi SK et al. Three-dimensional fuzzy graphene ultra-microelectrodes for subcellular electrical recordings. Nano Res. 13, 1444–1452 (2020).
90. Gong W. et al. Thermal transport in multidimensional silicon-graphene hybrid nanostructures. ACS Appl. Mater. Interfaces 13, 50206–50212 (2021). [PubMed: 34662104]
91. Huang X. & El-Sayed MA Gold nanoparticles: Optical properties and implementations in cancer diagnosis and photothermal therapy. J. Adv. Res 1, 13–28 (2010).
92. Mie G. Contributions to the optics of turbid media, particularly of colloidal metal solutions. Ann. Phys 25, 377–445 (1976).
93. Papavassiliou GC Optical properties of small inorganic and organic metal particles. Prog. Solid. State Chem. 12, 185–271 (1979).
94. Link S. & El-Sayed MA Size and temperature dependence of the plasmon absorption of colloidal gold nanoparticles. J. Phys. Chem. B 103, 4212–4217 (1999).
95. Chen H. et al. Understanding the photothermal conversion efficiency of gold nanocrystals. Small 6, 2272–2280 (2010). [PubMed: 20827680]
96. Lee K-S & El-Sayed MA Dependence of the enhanced optical scattering efficiency relative to that of absorption for gold metal nanorods on aspect ratio, size, end-cap shape, and medium refractive index. J. Phys. Chem. B 109, 20331–20338 (2005). [PubMed: 16853630]
97. Anayee M. et al. Role of acid mixtures etching on the surface chemistry and sodium ion storage in Ti3C2Tx MXene. Chem. Commun 56, 6090–6093 (2020).
98. Maleski K, Shuck CE, Fafarman AT & Gogotsi Y. The broad chromatic range of two-dimensional transition metal carbides. Adv. Opt. Mater 9, 2001563 (2021).
99. Lin H. et al. A 90-nm-thick graphene metamaterial for strong and extremely broadband absorption of unpolarized light. Nat. Photonics 13, 270–276 (2019).
100. Campbell P. & Green MA Light trapping properties of pyramidally textured surfaces. J. Appl. Phys 62, 243–249 (1987).
101. Yablonovitch E. Statistical ray optics. J. Opt. Soc. Am 72, 899–907 (1982).
102. Dipalo M. et al. Intracellular action potential recordings from cardiomyocytes by ultrafast pulsed laser irradiation of fuzzy graphene microelectrodes. Sci. Adv 7, eabd5175 (2021).
103. Yong J. et al. Gold-nanorod-assisted near-infrared stimulation of primary auditory neurons. Adv. Healthc. Mater 3, 1862–1868 (2014). [PubMed: 24799427]

104. Jiang Y. et al. Nongenetic optical neuromodulation with silicon-based materials. Nat. Protoc 14, 1339–1376 (2019). [PubMed: 30980031] The article presents a detailed protocol for the characterization of the local temperature response of nanomaterials using micro-pipette and nano-pipette thermometry.
105. Tobías I, Cañizo CD & Alonso J. In Handbook of Photovoltaic Science and Engineering 255–306 (Wiley, 2003).
106. Walter MG et al. Solar water splitting cells. Chem. Rev 110, 6446–6473 (2010). [PubMed: 21062097]
107. Su Y. et al. Gold nanoparticles-decorated silicon nanowires as highly efficient near-infrared hyperthermia agents for cancer cells destruction. Nano Lett. 12, 1845–1850 (2012). [PubMed: 22401822]
108. Gao M, Zhu L, Peh CK & Ho GW Solar absorber material and system designs for photothermal water vaporization towards clean water and energy production. Energy Environ. Sci 12, 841–864 (2019).
109. Hao J. et al. High performance optical absorber based on a plasmonic metamaterial. Appl. Phys. Lett 96, 251104 (2010).
110. Li R, Zhang L, Shi L. & Wang P. MXene Ti3C2: an effective 2D light-to-heat conversion material. ACS Nano 11, 3752–3759 (2017). [PubMed: 28339184]
111. Lee U, Yoo C-J, Kim Y-J & Yoo Y-M Cytotoxicity of gold nanoparticles in human neural precursor cells and rat cerebral cortex. J. Biosci. Bioeng 121, 341–344 (2016). [PubMed: 26277219]
112. Sani A, Cao C. & Cui D. Toxicity of gold nanoparticles (AuNPs): a review. Biochem. Biophys. Rep 26, 100991 (2021). [PubMed: 33912692]
113. Eom K. et al. Enhanced infrared neural stimulation using localized surface plasmon resonance of gold nanorods. Small 10, 3853–3857 (2014). [PubMed: 24975778] This article demonstrates photothermal excitation of the sciatic nerve using pulsed infrared illumination of interfaced plasmonic gold nanorods.
114. Lewinski N, Colvin V. & Drezek R. Cytotoxicity of nanoparticles. Small 4, 26–49 (2008). [PubMed: 18165959]
115. Tosheva KL, Yuan Y, Pereira PM, Culley S. & Henriques R. Between life and death: strategies to reduce phototoxicity in super-resolution microscopy. J. Phys. D Appl. Phys 53, 163001 (2020). [PubMed: 33994582]
116. Stockley JH et al. Surpassing light-induced cell damage in vitro with novel cell culture media. Sci. Rep 7, 849 (2017). [PubMed: 28405003]
117. Kuse Y, Ogawa K, Tsuruma K, Shimazawa M. & Hara H. Damage of photoreceptor-derived cells in culture induced by light emitting diode-derived blue light. Sci. Rep 4, 5223 (2014). [PubMed: 24909301]
118. Lim GP et al. Cytotoxicity of MXene-based nanomaterials for biomedical applications: a mini review. Environ. Res 201, 111592 (2021). [PubMed: 34175291]
119. Matino L, Rastogi SK, Garma LD, Cohen-Karni T. & Santoro F. Characterization of the coupling between out-of-plane graphene and electrogenic cells. Adv. Mater. Interfaces 7, 2000699 (2020).
120. Mullick Chowdhury S. et al. Cell specific cytotoxicity and uptake of graphene nanoribbons. Biomaterials 34, 283–293 (2013). [PubMed: 23072942]
121. Li Z. et al. Cellular level biocompatibility and biosafety of ZnO nanowires. J. Phys. Chem C. 112, 20114–20117 (2008).
122. Jastrzębska A. et al. In vitro studies on cytotoxicity of delaminated Ti3C2 MXene. J. Hazard. Mater 339, 1–8 (2017). [PubMed: 28601597]
123. Dai C. et al. Biocompatible 2D titanium carbide (MXenes) composite nanosheets for pH-responsive MRI-guided tumor hyperthermia. Chem. Mater 29, 8637–8652 (2017).
124. Zhang L. et al. Mechanisms of reactive oxygen species generated by inorganic nanomaterials for cancer therapeutics. Front. Chem 9, 630969 (2021). [PubMed: 33816437]
125. Bergamini CM, Gambetti S, Dondi A. & Cervellati C. Oxygen, reactive oxygen species and tissue damage. Curr. Pharm. Des 10, 1611–1626 (2004). [PubMed: 15134560]

126. Shields HJ, Traa A. & Van Raamsdonk JM Beneficial and detrimental effects of reactive oxygen species on lifespan: a comprehensive review of comparative and experimental studies. Front. Cell Dev. Biol 9, 628157 (2021). [PubMed: 33644065]

127. Yarmolenko PS et al. Thresholds for thermal damage to normal tissues: an update. Int. J. Hyperth 27, 320–343 (2011).

128. Sapareto SA & Dewey WC Thermal dose determination in cancer therapy. Int. J. Radiat. Oncol. Biol. Phys 10, 787–800 (1984). [PubMed: 6547421]

129. Dewhirst MW, Viglianti B, Lora-Michiels M, Hanson M. & Hoopes P. Basic principles of thermal dosimetry and thermal thresholds for tissue damage from hyperthermia. Int. J. Hyperth 19, 267–294 (2003).

130. Sharma H. Hyperthermia influences excitatory and inhibitory amino acid neurotransmitters in the central nervous system. An experimental study in the rat using behavioural, biochemical, pharmacological, and morphological approaches. J. Neural Transm. 113, 497–519 (2006). [PubMed: 16550328]

131. Liebregts MT, McLachlan RS & Leung LS Hyperthermia induces age-dependent changes in rat hippocampal excitability. Ann. Neurol 52, 318–326 (2002). [PubMed: 12205644]

132. Johannsmeier S. et al. Gold nanoparticle-mediated laser stimulation induces a complex stress response in neuronal cells. Sci. Rep 8, 6533 (2018). [PubMed: 29695746]

133. Battaglini M. et al. Polydopamine nanoparticles as an organic and biodegradable multitasking tool for neuroprotection and remote neuronal stimulation. ACS Appl. Mater. Interfaces 12, 35782–35798 (2020). [PubMed: 32693584]

134. Carvalho-de-Souza JL et al. Cholesterol functionalization of gold nanoparticles enhances photoactivation of neural activity. ACS Chem. Neurosci 10, 1478–1487 (2018).

135. DiFrancesco ML et al. A hybrid P3HT-graphene interface for efficient photostimulation of neurons. Carbon 162, 308–317 (2020).

136. Yoo S, Hong S, Choi Y, Park JH & Nam Y. Photothermal inhibition of neural activity with near-infrared-sensitive nanotransducers. ACS Nano 8, 8040–8049 (2014). [PubMed: 25046316] This article reports that photothermal inhibition induced using nanoparticles (gold nanorods) can be tuned by modulating the illumination conditions.

137. Lee JW, Jung H, Cho HH, Lee JH & Nam Y. Gold nanostar-mediated neural activity control using plasmonic photothermal effects. Biomaterials 153, 59–69 (2018). [PubMed: 29102745]

138. Kang H, Lee G-H, Jung H, Lee JW & Nam Y. Inkjet-printed biofunctional thermo-plasmonic interfaces for patterned neuromodulation. ACS Nano 12, 1128–1138 (2018). [PubMed: 29402086]

139. Feyen P. et al. Light-evoked hyperpolarization and silencing of neurons by conjugated polymers. Sci. Rep 6, 22718 (2016). [PubMed: 26940513]

140. Lavoie-Cardinal F, Salesse C, Bergeron É, Meunier M. & De Koninck P. Gold nanoparticle-assisted all optical localized stimulation and monitoring of Ca2+ signaling in neurons. Sci. Rep 6, 20619 (2016). [PubMed: 26857748]

141. Eom K. et al. Photothermal activation of astrocyte cells using localized surface plasmon resonance of gold nanorods. J. Biophotonics 10, 486–493 (2017). [PubMed: 28164459]

142. Eom K. et al. Synergistic combination of near-infrared irradiation and targeted gold nanoheaters for enhanced photothermal neural stimulation. Biomed. Opt. Express 7, 1614–1625 (2016). [PubMed: 27446678]

143. Nakatsuji H. et al. Thermosensitive ion channel activation in single neuronal cells by using surface-engineered plasmonic nanoparticles. Angew. Chem. Int. Ed 54, 11725–11729 (2015).

144. Paviolo C, Haycock JW, Cadusch PJ, McArthur SL & Stoddart PR Laser exposure of gold nanorods can induce intracellular calcium transients. J. Biophotonics 7, 761–765 (2014). [PubMed: 23798060]

145. Grienberger C. & Konnerth A. Imaging calcium in neurons. Neuron 73, 862–885 (2012). [PubMed: 22405199]

146. Jiang Y. et al. Heterogeneous silicon mesostructures for lipid-supported bioelectric interfaces. Nat. Mater 15, 1023–1030 (2016). [PubMed: 27348576]

147. Miyako E. et al. Photofunctional nanomodulators for bioexcitation. Angew. Chem 126, 13337–13341 (2014).
148. Sakmann B. & Neher E. Patch clamp techniques for studying ionic channels in excitable membranes. Annu. Rev. Physiol 46, 455–472 (1984). [PubMed: 6143532]
149. Tang M. et al. Injectable black phosphorus nanosheets for wireless nongenetic neural stimulation. Small 10.1002/smll.202105388 2021).
150. Jiang S, Wu X, Rommelfanger NJ, Ou Z. & Hong G. Shedding light on neurons: optical approaches for neuromodulation. Natl Sci. Rev 9, nwac007 (2022).
151. Hong G, Antaris AL & Dai H. Near-infrared fluorophores for biomedical imaging. Nat. Biomed. Eng 1, 0010 (2017).
152. Bashkatov AN, Genina E, Kochubey V. & Tuchin V. Optical properties of human skin, subcutaneous and mucous tissues in the wavelength range from 400 to 2000 nm. J. Phys. D Appl. Phys 38, 2543 (2005).
153. Mie G. Beiträge zur Optik trüber Medien, speziell kolloidaler Metallösungen. Ann. Phys 330, 377–445 (1908).
154. Rayleigh JWSB On the Scattering of Light by Small Particles (Cambridge University Press, 1871).
155. Jung H. & Nam Y. Optical recording of neural responses to gold-nanorod mediated photothermal neural inhibition. J. Neurosci. Methods 373, 109564 (2022). [PubMed: 35292307]
156. An Y. & Nam Y. Closed-loop control of neural spike rate of cultured neurons using a thermoplasmonics-based photothermal neural stimulation. J. Neural Eng. 18, 066002 (2021).
157. Lee SE, Liu GL, Kim F. & Lee LP Remote optical switch for localized and selective control of gene interference. Nano Lett. 9, 562–570 (2009). [PubMed: 19128006]
158. Wijaya A, Schaffer SB, Pallares IG & Hamad-Schifferli K. Selective release of multiple DNA oligonucleotides from gold nanorods. ACS Nano 3, 80–86 (2009). [PubMed: 19206252]
159. Carrow JK et al. Photothermal modulation of human stem cells using light-responsive 2D nanomaterials. Proc. Natl Acad. Sci. USA 117, 13329–13338 (2020). [PubMed: 32461372] This article demonstrates photothermal modulation of gene expression and cellular functions in human stem cells using 2D transition metal dichalcogenides such as MoS_2.
160. Fricker M, Tolkovsky AM, Borutaite V, Coleman M. & Brown GC Neuronal cell death. Physiol. Rev 98, 813–880 (2018). [PubMed: 29488822]
161. Lodola F. et al. Conjugated polymers optically regulate the fate of endothelial colony-forming cells. Sci. Adv 5, eaav4620 (2019).
162. Milos F. et al. High aspect ratio and light-sensitive micropillars based on a semiconducting polymer optically regulate neuronal growth. ACS Appl. Mater. Interfaces 13, 23438–23451 (2021). [PubMed: 33983012]
163. Aziz IA et al. Light-triggered electron transfer between a conjugated polymer and cytochrome C for optical modulation of redox signaling. iScience 23, 101091 (2020). [PubMed: 32438318]
164. Huh D, Hamilton GA & Ingber DE From 3D cell culture to organs-on-chips. Trends Cell Biol. 21, 745–754 (2011). [PubMed: 22033488]
165. Lee A. et al. 3D bioprinting of collagen to rebuild components of the human heart. Science 365, 482–487 (2019). [PubMed: 31371612]
166. Kalmykov A. et al. Bioelectrical interfaces with cortical spheroids in three-dimensions. J. Neural Eng. 18, 055005 (2021).
167. Andersson HA, Kim Y-S, O'Neill BE, Shi Z-Z & Serda RE HSP70 promoter-driven activation of gene expression for immunotherapy using gold nanorods and near infrared light. Vaccines 2, 216–227 (2014). [PubMed: 25328682]
168. Chen X, Chen Y, Xin H, Wan T. & Ping Y. Near-infrared optogenetic engineering of photothermal nanoCRISPR for programmable genome editing. Proc. Natl Acad. Sci. USA 117, 2395–2405 (2020). [PubMed: 31941712]
169. Fisher RS & Velasco AL Electrical brain stimulation for epilepsy. Nat. Rev. Neurol 10, 261–270 (2014). [PubMed: 24709892]

170. Đerek V, Rand D, Migliaccio L, Hanein Y. & Głowacki ED Untangling photofaradaic and photocapacitive effects in organic optoelectronic stimulation devices. Front. Bioeng. Biotechnol 8, 284 (2020). [PubMed: 32363183]
171. Medagoda DI & Ghezzi D. Organic semiconductors for light-mediated neuromodulation. Commun. Mater 2, 111 (2021).
172. Nair V. et al. Laser writing of nitrogen-doped silicon carbide for biological modulation. Sci. Adv 6, eaaz2743 (2020).
173. Alberts B. Molecular Biology of the Cell (Garland Science, 2008).
174. Nicholls JG, Martin AR, Wallace BG & Fuchs PA From Neuron to Brain. Vol. 271 (Sinauer Associates Sunderland, 2001).
175. Paulsen CE, Armache J-P, Gao Y, Cheng Y. & Julius D. Structure of the TRPA1 ion channel suggests regulatory mechanisms. Nature 520, 511–517 (2015). [PubMed: 25855297]
176. Crunelli V. & Leresche N. A role for GABAB receptors in excitation and inhibition of thalamocortical cells. Trends Neurosci. 14, 16–21 (1991). [PubMed: 1709527]
177. Mitragotri S, Burke PA & Langer R. Overcoming the challenges in administering biopharmaceuticals: formulation and delivery strategies. Nat. Rev. Drug Discov. 13, 655–672 (2014). [PubMed: 25103255]
178. Singh R. & Lillard JW Jr. Nanoparticle-based targeted drug delivery. Exp. Mol. Pathol 86, 215–223 (2009). [PubMed: 19186176]
179. Kim CY et al. Soft subdermal implant capable of wireless battery charging and programmable controls for applications in optogenetics. Nat. Commun 12, 535 (2021). [PubMed: 33483493]
180. Ausra J. et al. Wireless, battery-free, subdermally implantable platforms for transcranial and long-range optogenetics in freely moving animals. Proc. Natl Acad. Sci. USA 118, e2025775118 (2021). [PubMed: 34301889]
181. Reddy JW, Lassiter M. & Chamanzar M. Parylene photonics: a flexible, broadband optical waveguide platform with integrated micromirrors for biointerfaces. Microsyst. Nanoeng 6, 85 (2020). [PubMed: 34567695]
182. Scopelliti MG & Chamanzar M. Ultrasonically sculpted virtual relay lens for in situ microimaging. Light Sci. Appl 8, 65 (2019). [PubMed: 31645914]
183. Kim D. et al. Ultraflexible organic light-emitting diodes for optogenetic nerve stimulation. Proc. Natl Acad. Sci. USA 117, 21138–21146 (2020). [PubMed: 32817422]
184. Nel AE et al. Understanding biophysicochemical interactions at the nano–bio interface. Nat. Mater 8, 543–557 (2009). [PubMed: 19525947]
185. Petros RA & DeSimone JM Strategies in the design of nanoparticles for therapeutic applications. Nat. Rev. Drug Discov. 9, 615–627 (2010). [PubMed: 20616808]
186. Benfenati F. & Lanzani G. Clinical translation of nanoparticles for neural stimulation. Nat. Rev. Mater 6, 1–4 (2021).
187. Charbgoo F. et al. Gold nanoparticle should understand protein corona for being a clinical nanomaterial. J. Control. Rel 272, 39–53 (2018).

Box 1 Effects of transient temperature changes on cells

The cell membrane is composed of amphipathic lipids and functional proteins. Temperature-sensitive proteins can respond to external thermal stimuli to regulate cellular behaviour[173]. The following properties and temperature-responsive components of the cell membrane are important in the photothermal modulation of cellular electrophysiology.

Electrical properties

***V*r.** The membrane resting potential (V_r) is the potential difference across the cell membrane in the absence of electrical activity. Ionic concentrations, such as of Na^+, K^+, and Cl^-, are different between intracellular and extracellular environments owing to the selective permeability of the cell membrane. At the resting state, the Goldman–Hodgkin–Katz model describes the potential difference across the cell membrane as follows[49]:

$$V_r = \frac{RT}{F}\ln\left(\frac{p_K[K^+]_E + p_{Na}[Na^+]_E + p_{Cl}[Cl^-]_I}{p_K[K^+]_I + p_{Na}[Na^+]_I + p_{Cl}[Cl^-]_E}\right)$$

where R, T, F, p_i, E and I indicate the ideal gas constant, current temperature of the system, Faraday constant, permeability of ion i (i = Na^+, K^+ and Cl^-), and extracellular and intracellular ionic concentrations, respectively. For neurons, V_r generally lies between −85 mV and −60 mV without external stimulus[174].

***V*s.** The surface potential (V_s) is a result of charge accumulation at the inner and outer surfaces of the cell membrane. Ions adsorb on the phospholipid head following the Gouy–Chapman–Stern membrane biophysical model[22,42,43]. The asymmetrical adsorption of ions results in the surface potential.

***R*m.** R_m describes the resistive element in the cell membrane circuit; ion channels in the cell membrane provide a pathway for ionic conduction between intracellular and extracellular environments, which can be modelled as resistors[22,43].

***C*m.** C_m describes the capacitive element in the cell membrane circuit; the membrane bilayer can charge or discharge like a capacitor owing to a change in surface charge potential V_s(refs. [22,43]).

Temperature-activated TRP ion channels

Temperature-activated transient receptor potential (TRP) ion channels consist of six putative membrane-spanning units. Each unit has its own temperature sensitivity and corresponding threshold for opening and closing; for example, TRP vanilloid 1 (TRPV1) can be activated by temperatures equal to or higher than 42 °C. This leads to channel opening and Ca^{2+} influx, which triggers an action potential[55]. TRP ankyrin 1 (TRPA1) is also a rapid-response somatosensory ion channel that responds to thermal and chemical stimuli[32]. The temperature sensitivity and behavioural response of TRPA1 vary across species[175].

Electrophysiological phenomena

Action potential.

Refers to a rapid increase and subsequent decrease in potential across the cell membrane, triggered by the active flow of ions, such as Na^+ and K^+, across the cell membrane. An action potential can propagate along the dimensions of a cell and can be transmitted to other cells through neurotransmitters[173,174].

Cellular excitation.

Refers to the generation of an action potential. Any stimuli that cause the cell membrane potential to increase above the threshold (approximately −55 mV) triggers an influx of Na^+ through voltage-gated Na^+ channels resulting in depolarization[173,174].

Cellular inhibition.

Refers to the suppression of an action potential. Inhibition occurs through inhibitory interneuron transmitters (for example, γ-aminobutyric acid) that further reduce the cell membrane potential (hyperpolarization) by activating specific ion channels (for example, voltage-gated K^+ channels)[176]. An externally stimulated increase in membrane conductance can also result in hyperpolarization[139].

Box 2 Translational considerations

Cell-specific control

Targeted delivery of nanomaterials to specific neurons enables selective control of specific brain regions; for example, injecting nanoparticles to the motor cortex of the whisker region of rats results in whisker oscillation with light irradiation pulses[142]. Controlled site-specific injection of nanoparticles and mapping brain activity as a response to targeted modulation will increase our understanding of neural circuits[149]. However, the absence of precise control over the spatial distribution of nanomaterials in target tissues decreases the efficiency of photothermal modulation. Chemical modification of nanomaterials is a promising approach to targeting specific cell types in vitro that can be translated in vivo[39,134,140,142,143,177]; for example, nanomaterials can be functionalized with peptides, cell-surface receptors and antibodies to allow cell-specific binding[177,178].

Localized delivery of light pulses

Ideal photothermal stimulation approaches should facilitate localized delivery of light pulses with sufficient input energies in a minimally invasive manner. This can be achieved through miniaturized optoelectronic systems with high output energies and stable power supply (such as microscale, inorganic light-emitting diodes)[8,179,180]. Additionally, compact, soft and flexible polymer photonics[181] and ultrasonic steering of light could allow non-invasive light delivery[182]. Such systems could be coupled with photothermally active nanomaterials to enable clinical translation[179,180,183]. In addition, combined approaches will expand the nanomaterial library for deep-tissue neuromodulation without the need for NIR-active nanomaterials.

Engineering biointerface stability

Photothermal modulation heavily relies on the biointerface between the cell membrane and nanomaterials. Temporal stability of the biointerface is therefore crucial for in vivo applications. Numerous biocompatible and bioresorbable materials, such as Si-based materials, have been developed for transient bioelectronic applications[6,37], and a library of materials has been evaluated for long-term biointerfaces, including graphene-based materials[9]. Engineering the physical structure and topography of these materials can alter their photothermal response and expand the library of photothermally active nanomaterials. Tuning the surface and compositional chemistry of the nanomaterials can further facilitate phagocytosis and biodegradation[4,5,184,185]. However, nanomaterials are rapidly coated by a protein corona when injected into the body[186], which negatively affects photothermal energy transduction. Surface functionalization with molecules (such as PEG), zwitterions (such as poly(carboxybetaine)) and proteins (such as albumin) can minimize the formation of protein corona[187]. However, new strategies for surface functionalization that do not affect optical and photothermal properties need to be developed.

Key points

- Nanomaterial-assisted photothermal modulation is a remote, non-genetic technique for the manipulation of neural activity with high spatiotemporal resolution and specificity by inducing a rapid temperature increase at the cell–nanomaterial interface.
- The fundamental properties of photothermally active nanomaterials (size, dimension, optical absorbance and photothermal energy conversion) and illumination conditions dictate application-specific material selection.
- Altering light illumination conditions (pulse width, power density and spot size) allows control of neural electrophysiology (excitation and inhibition) and cellular signalling pathways.
- Evaluation of the cytotoxicity of nanomaterials, phototoxicity of light illumination and local temperature increases is necessary for the safe translation of transient and long-term photothermal modulation.

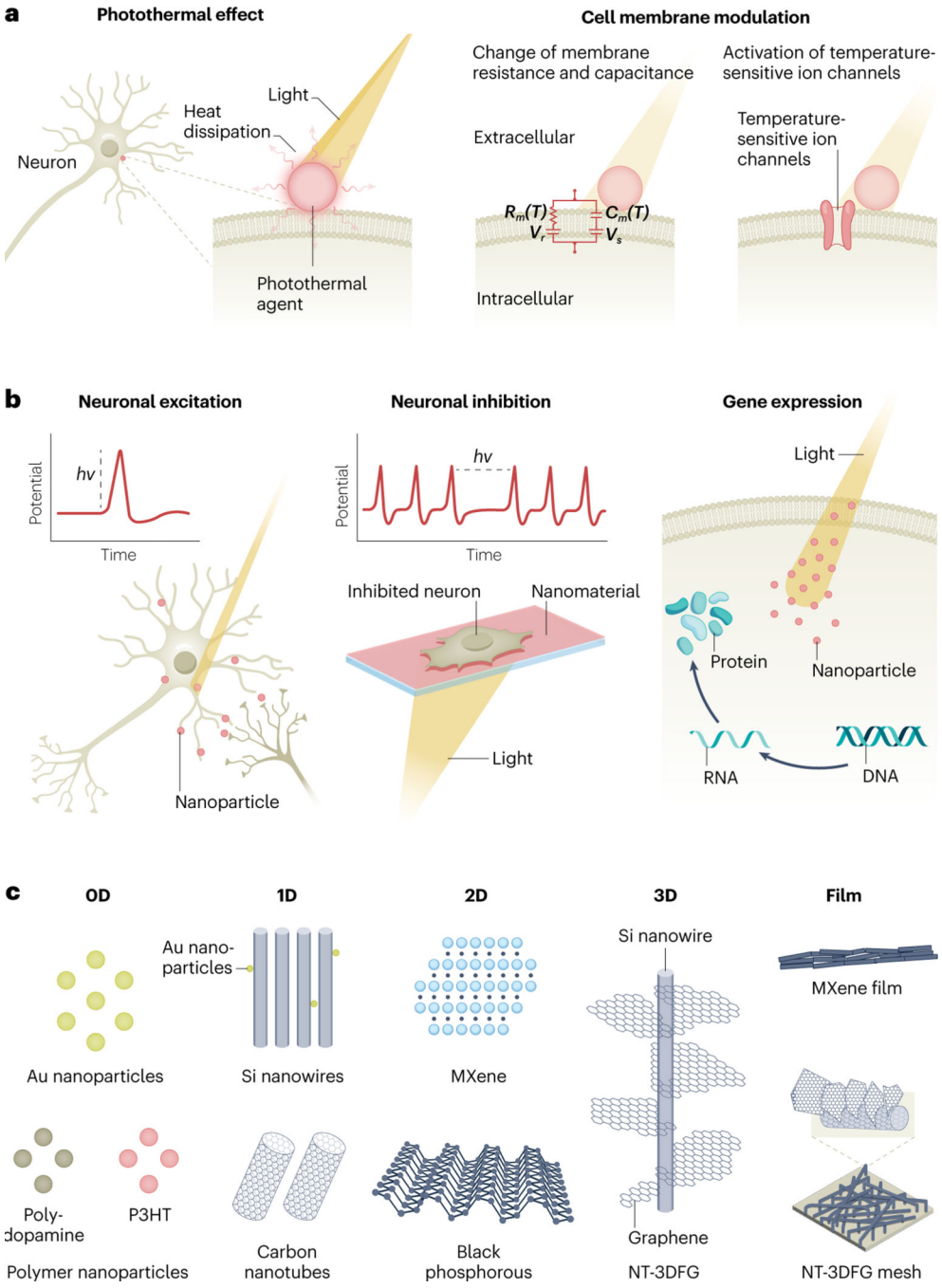

Fig. 1 |. Mechanisms of photothermal modulation.

a, Proposed mechanisms of photothermal modulation. Step 1: Nanoparticles interfaced with the cell membrane cause localized release of thermal energy at the cell membrane when exposed to laser irradiation. Step 2: The cell membrane is modelled as a combination of electronic elements: $R_m(T)$ and $C_m(T)$, V_s and V_r, which are the cell membrane-resistive and capacitive elements as a function of temperature, net surface potential, and resting potential, respectively. Local temperature changes affect membrane resistance and capacitance. Temperature-sensitive ion channels at the cell membrane also have an important role in

photothermal modulation. **b**, Applications of photothermal neural modulation. Illuminating light at the interface between photothermal nanomaterials and cells enables switching between neural excitation and inhibition as well as modulation of gene expression and protein translation. **c**, Photothermally active nanomaterials of different dimensions (from zero-dimensional (0D) to three-dimensional (3D)) can be used in the form of clusters or films. The diversity in material dimensions and formats allows the formation of various biointerfaces. Nanowire-templated 3D fuzzy graphene (NT-3DFG) schematic is adapted with permission from ref. [87]. Copyright 2019 American Chemical Society. NT-3DFG mesh schematic is adapted with permission from ref. [86]. Copyright 2017 American Chemical Society.

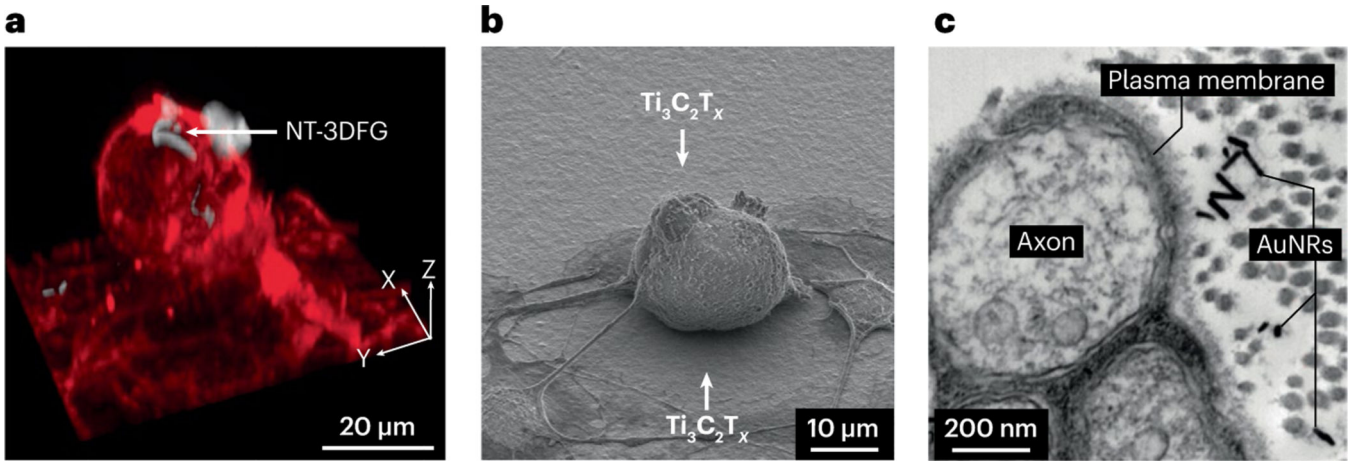

Fig. 2 |. Nanomaterial–cell biointerfaces.

a, Nanowire-templated three-dimensional fuzzy graphene (NT-3DFG) adheres to the cell membrane of dorsal root ganglion (DRG) neurons. A three-dimensional reconstruction of the fluorescence image presents a representative DRG neuron labelled with plasma membrane stain (red, labelled with CellMask deep red plasma membrane stain) and interfaced with NT-3DFG (white). **b**, DRG neurons interact with a titanium carbide ($Ti_3C_2T_x$, where T_x indicates the surface termination functional group) film. Representative scanning electron microscopy image of DRG neurons seeded on a $Ti_3C_2T_x$ film (background of the image). **c**, Transmission electron microscopy image of a cross-sectional view of rat sciatic nerve after injection of Au nanorods (AuNRs), which are located near the surface of the plasma membrane of the axon. Part **a** is adapted with permission from ref. [29], National Academy of Sciences. Part **b** is adapted with permission from ref. [40], Wang et al. Part **c** is adapted with permission from ref. [113], Wiley.

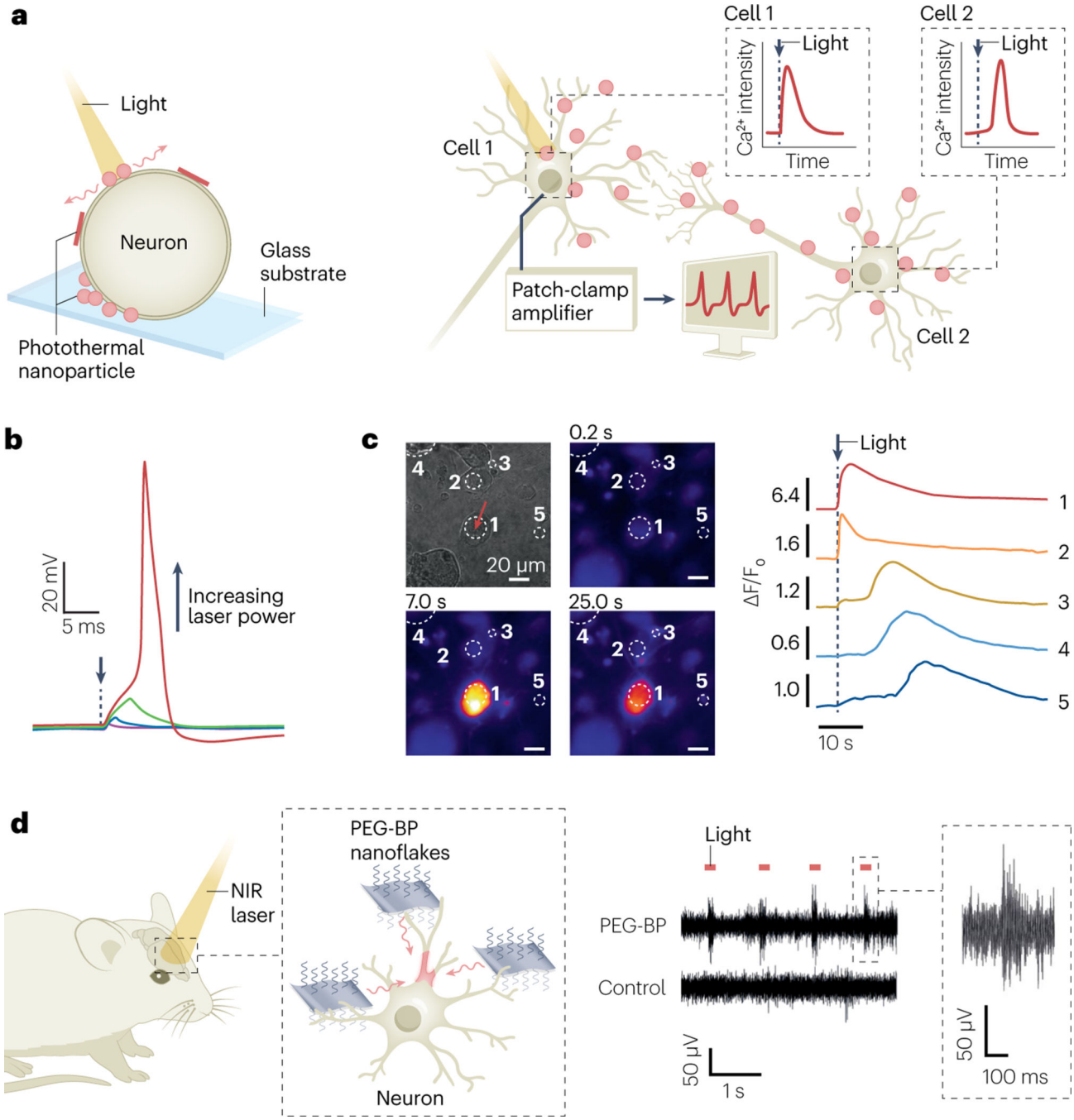

Fig. 3 |. In vitro and in vivo neural excitation with photothermally active nanomaterials.
a, Biointerface between multidimensional nanoparticles and a neuron for photothermal stimulation (left panel). Experimental setup for recording electrical activities of neural networks induced by photothermal excitation (right panel). **b**, Representative action potential of current-clamped dorsal root ganglion (DRG) neurons interfaced with nanowire-templated three-dimensional fuzzy graphene (NT-3DFG) and irradiated with a 405 nm laser of different powers (1.2 ms, 1.45 mW (violet), 1.73 mW (blue), 2.28 mW (green), and 3.02 mW (red)). Purple arrow indicates the applied laser pulse starting point. **c**, Photothermal

excitation of DRG neural network using titanium carbide ($Ti_3C_2T_x$) MXene. Bright-field and time series fluorescence images of a representative DRG neuron interfaced with a $Ti_3C_2T_x$ film and irradiated with laser (635 nm, 1 ms, 5.7 J cm^{-2} per pulse) at $t = 5.6$ s (left panel). Normalized Ca^{2+} fluorescence intensity as a function of time for the regions of interest marked in the left panel (right panel). Red arrow denotes the starting point of the applied laser pulse ($t = 5.6$ s). 1–5 indicate the DRG neurons highlighted in the left panel. **d**, In vivo neural excitation using polyethylene glycol (PEG)-modified black phosphorus (PEG-BP) nanoflakes in rat brains. A schematic of PEG-BP nanoflakes as a heat transducer for wireless neural stimulation (left panel). Representative recordings of spiking activities in cells in response to pulses of a near-infrared (NIR) light (808 nm, 30 ms, 0.15 J cm^{-2} per pulse, 1 Hz) with/without PEG-BP nanoflakes (right panel). Part **a** is adapted with permission from ref. [29], National Academy of Sciences. Part **b** is reproduced with permission from ref. [29], Rastogi et al. Part **c** is adapted with permission from ref. [40], Wang et al. Part **d** is reproduced with permission from ref. [149], Wiley.

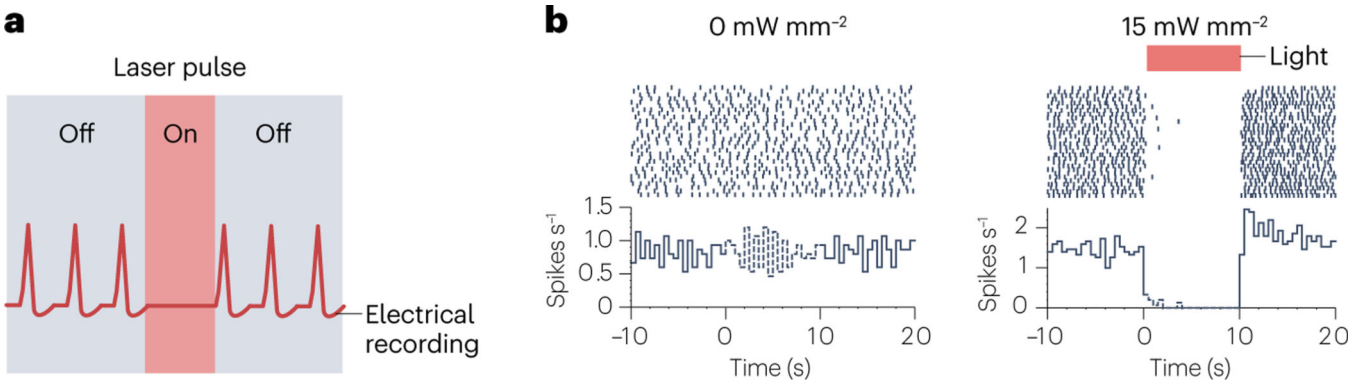

Fig. 4 |. Photothermal neural inhibition with nanomaterials.

a, Schematic illustrating the input laser pulse responsible for the measured output electrical recordings from a neuron under photothermal inhibition. **b**, Inhibition of neural activity with near-infrared-sensitive Au nanorods. (I) Peri-event raster plots and histograms for neural activity with and without 785 nm illumination at 0 mW mm^{-2} (left panel) and 15 mW mm^{-2} (15 J cm^{-2}) (10 s light on and 20 s light off) (right panel). Part **b** is adapted with permission from ref. [136]. Copyright 2014 American Chemical Society.

Table 1 |

Photothermal response of nanomaterials

Material	Laser wavelength (λ, nm)	Incident energy	Temperature change (K)	Synthesis	Advantages	Challenges	Ref.
Au nanoparticles							
Silica-coated AuNRs	785	42 J cm^{-2} at 780 nm	~3.5 (NR clusters)	Liquid process	Long-term injection and implantation for neural modulation	High cost	103
Ts1-functionalized AuNPs	532	31 J cm^{-2} at 532 nm	~2 (NP clusters)	Liquid process			39
Si nanostructures							
Mesostructured Si film	Visible range absorber	0.89 J cm^{-2} at 532 nm	~5.8 (film)	Liquid process	Neural modulation at multiple scales	Requires high input energies to reach excitation thresholds	146
i-SiNWs	Visible range absorber	2398 J cm^{-2} at 532 nm	~5.4 (individual wire)	CVD			37
Au-decorated SiNWs	Visible range absorber	240 J cm^{-2} at 532 nm	~2 (individual wire)	CVD			31
C nanostructures							
NT-3DFG	Broadband absorber	3.18 J cm^{-2} at 635 nm	~6 (individual wire)	CVD	Long-term neural modulation with low-incident energy	Scalability of production	29
MXenes							
$Ti_3C_2T_x$ (flake)	780	3.18 J cm^{-2} at 808 nm	~3.3 (individual flake)	Liquid exfoliation	Neural modulation with low-incident energies across different scales	Instability owing to surface oxidation and degradation in physiological environment	40
$Ti_3C_2T_x$ (film)	780	3.18 J cm^{-2} at 635 nm	~11.7 (film)				
BP							
PEG-functionalized BP	300	0.02 J cm^{-2} at 808 nm	~4 (100 μg ml^{-1} suspension)	Liquid exfoliation	Neural modulation with low-incident energy across different scales	Instability owing to degradation in physiological environment and low activity in NIR window	149
Polymer nanostructures							
Semiconducting polymer nano-bioconjugates	766	360 J cm^{-2} at 808 nm	~50 (18 μg ml^{-1} suspension)	Liquid-based reaction	High biocompatibility; can be implanted or injected	Instability owing to degradation; limited efficiency of photothermal energy conversion	41
Lipid-coated polydopamine nanoparticles	870	84.95 J cm^{-2} at 808 nm	~2.7 (100 μg ml^{-1} suspension)	Liquid-based reaction			133
MINDS	~1,000	4 J cm^{-2} at 1,064 nm	~40 (1.8 μg ml^{-1} suspension)	Liquid-based reaction			53

Material	Laser wavelength (λ, nm)	Incident energy	Temperature change (K)	Synthesis	Advantages	Challenges	Ref.
Poly(3-hexylthiophene) film	475	0.11 J cm^{-2} at 435 nm	~3 (film)	Spin coating			52

BP, black phosphorus; CVD, chemical vapour deposition; i-SiNWs; intrinsic Si nanowires; MINDS, macromolecular NIR-II-absorbing polymeric nanoparticles; NIR, near-infrared; NPs, nanoparticles; NRs, nanorods; NT-3DFG, nanowire-templated three-dimensional fuzzy graphene; NW, nanowire; PEG, polyethylene glycol; $Ti_3C_2T_x$; titanium carbide, where *x* indicates the surface termination functional group; Ts1, neurotoxin from *Tityus serrulatus*.